CLEAN ENERGY TECHNOLOGIES JOURNAL

YTU PRESS

www.cetj.yildiz.edu.tr

CLEAN ENERGY TECHNOLOGIES JOURNAL

CLEAN ENERGY TECHNOLOGIES JOURNAL

About Us

Clean Energy Technologies Journal is an open access, transdisciplinary, peer-reviewed international journal focusing on sourcing, transforming, transporting, delivering and using the energy in a sustainable and clean way. The role of energy in the progress and development of civilization is undeniable. However, in order for this progress to continue, it is of great importance that energy be clean and sustainable. **Clean Energy Technologies Journal** is a platform to debate issues of providing energy in sustainable and a clean way.

The journal will present and disseminate the innovations and practical achievements in the field of clean energy, and to provide core academic resources for experts and scholars engaged in energy research.

Clean Energy Technologies Journal is indexed in IdealOnline, Asian Science Citation Index, Open Ukranian Citation Index, Scilit and Gale Cengage.
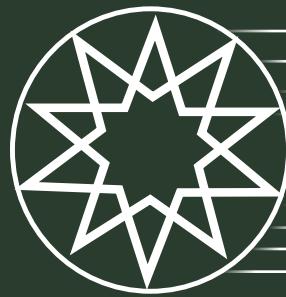
Ethics & Policies

Advertisement Policy

Clean Energy Technologies Journal does not accept advertisements; the journal is sponsored by the Yildiz Technical University.

Archiving Policy

The content published by the Clean Energy Technologies Journal is electronically preserved by using Internet archive.

Authorship Policy

All statements and opinions expressed in the manuscripts published in the Clean Energy Technologies Journal reflect the views of the author(s).

Each individual listed as an author should fulfill the authorship criteria. The authorship should be based on the following 4 criteria:

Substantial contributions to the conception or design of the work, or the acquisition, analysis, or interpretation of data for the work; AND

Drafting the work or revising it critically for important intellectual content; AND

Final approval of the version to be published; AND

Agreement to be accountable for all aspects of the work in ensuring that questions related to the accuracy or integrity of any part of the work are appropriately investigated and resolved.

In addition to being accountable for their own work, authors should have confidence in the integrity of the contributions of their co-authors and each author should be able to identify which co-authors are responsible for other parts of the work.

All of those designated as authors should meet all four criteria for authorship, and all who meet the four criteria should be identified as authors. Those who provided a contribution but do not meet all four criteria should be recognized separately on the title page and in the Acknowledgements section at the conclusion of the manuscript.

The Clean Energy Technologies Journal requires that corresponding authors submit a signed and scanned version of the authorship contribution form (available for download through) during the initial submission process in order to appropriately indicate and observe authorship rights and to prevent ghost or honorary authorship. Please note that the list of authors on the final manuscript will be presented in the order provided on this form. If the editorial board suspects a case of "gift authorship," the submission will be rejected without further review. As part of the submission of the manuscript, the corresponding author should also send a short statement declaring that they accept all responsibility for authorship during the submission and review stages of the manuscript.

Complaint and Appeal Policy

Appeal and complaint cases are handled within the scope of COPE guidelines by the Editorial Board of the journal. Appeals should be based on the scientific content of the manuscript. The final decision on the appeal and complaint is made by Editor in Chief. An Ombudsperson or the Ethical Editor is assigned to resolve cases that cannot be resolved internally. Authors should get in contact with the Editor in Chief regarding their appeals and complaints via e-mail at kare@karepb.com

Corrections Policy

If the editors or publisher learn from a third party that a published work contains a material error or inaccuracy, the authors must promptly correct or retract the article or provide the journal editors with evidence of the accuracy of the article.

Ethics Policy

The Editorial Board of the Clean Energy Technologies Journal and the Publisher adheres to the principles of the Council of Science Editors (CSE), the Committee on Publication Ethics (COPE), the International Council of Medical Journal Editors (ICMJE), the World Association of Medical Editors (WAME), the US National Library of Medicine (NLM), and the European Association of Science Editors (EASE).

If the submitted manuscript does not include ethics committee approval, it will be reviewed according to COPE's guideline (Guidance for Editors: Research, Audit and Service Evaluations). If the study should have ethical approval, authors will be asked to provide ethical approval in order to proceed the review process. If they cannot provide ethical approval, their manuscript will be rejected and also their institutions and when needed, the related bodies in their country will be informed that such studies must have ethics committee approval. If they provide approval, review of the manuscript will continue.

If the study does not need ethics committee approval after the editorial board's review, the authors will be asked to provide an ethics committee approval or a document given by a related independent committee that indicates the study does not need ethics committee approval according to the research integrity rules in their country. If the authors provide either an approval or a document showing that ethics approval is not needed, the review process can be continued. If the authors cannot provide either documents, the manuscript may be rejected.
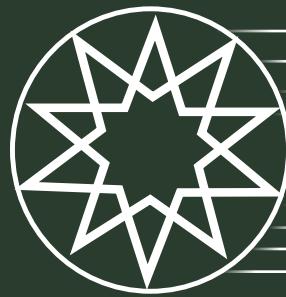
Ethics & Policies

Fee Waiver Policy

There is no fee waiver.

Funding Sources Policy

All authors are required to declare what support they received to carry out their research. Declaring funding sources acknowledges funders' contributions, fulfills funding requirements, and promotes greater transparency in the research process.

Each author must individually declare all sources of funding received for the research submitted to the journal. This information includes the name of granting agencies, grant numbers, and a description of each funder's role. If the funder has played no role in the research, this must be stated as well.

Authors are not required to provide the complete list of every single grant that supports them if the grant is not related to the research published.

Licenses and Copyright Policy

Authors publishing with the journal retain the copyright to their work licensed under the Creative Commons Attribution-NonCommercial 4.0 International license (CC BY-NC 4.0) and grant the Publisher non-exclusive commercial right to publish the work. CC BY-NC 4.0 license permits unrestricted, non-commercial use, distribution, and reproduction in any medium, provided the original work is properly cited.

Open Access Policy

The Clean Energy Technologies Journal supports the Budapest Open Access Initiative statement of principles that promotes free access to research literature. The declaration defines open access to academic literature as free availability on the internet, permitting users to read, record, copy, print, search, or link to the full text, examine them for indexing, use them as data for software or other lawful purposes without financial, legal, or technical barriers. Information sharing represents a public good, and is essential to the advancement of science. Therefore, articles published in this journal are available for use by researchers and other readers without permission from the author or the publisher provided that the author and the original source are cited. The articles in the Clean Energy Technologies Journal are accessible through search engines, websites, blogs, and other digital platforms. Additional details on the Budapest Open Access Initiative and their guidelines are available at https://www.budapestopenaccessinitiative.org.

Open Access Policy is based on rules of Budapest Open Access Initiative the Clean Energy Technologies Journal applies the Creative Commons Attribution-NonCommercial 4.0 International (CC BY-NC 4.0) license to articles we publish. If you submit your paper for publication, you agree to have the CC BY-NC 4.0 license applied to your work. Under this Open Access license, you as the author agree that anyone can copy, distribute or reuse the content of your article for non-commercial purposes for free as long as the author and original source are properly cited. The corresponding author must sign the Creative Commons License Agreement after their articles are accepted.

Open Access Statement

The journal is an open access journal and all content is freely available without charge to the user or his/her institution. Except for commercial purposes, users are allowed to read, download, copy, print, search, or link to the full texts of the articles in this journal without asking prior permission from the publisher or the author. This is in accordance with the BOAI definition of open access. The open access articles in the journal are licensed under the terms of the Creative Commons Attribution-NonCommercial 4.0 International (CC BY-NC 4.0) license.

Peer Review Policy

Only those manuscripts approved by its every individual author and that were not published before in or sent to another journal, are accepted for evaluation.

Submitted manuscripts that pass preliminary control are scanned for plagiarism using iThenticate software. After plagiarism check, the eligible ones are evaluated by Editor-in-Chief for their originality, methodology, the importance of the subject covered and compliance with the journal scope. Editor-in-Chief evaluates manuscripts for their scientific content without regard to ethnic origin, gender, sexual orientation, citizenship, religious belief or political philosophy of the authors and ensures a fair double-blind peer review of the selected manuscripts.

The selected manuscripts are sent to at least two national/international referees for evaluation and publication decision is given by Editor-in-Chief upon modification by the authors in accordance with the referees' claims.

Editor-in-Chief does not allow any conflicts of interest between the authors, editors and reviewers and is responsible for final decision for publication of the manuscripts in the Journal.

Reviewers' judgments must be objective. Reviewers' comments on the following aspects are expected while conducting the review.
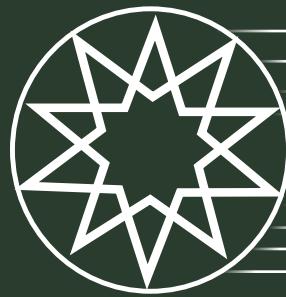
Volume 3 Number 2 Year 2025

Ethics & Policies

- Does the manuscript contain new and significant information?
- Does the abstract clearly and accurately describe the content of the manuscript?
- Is the problem significant and concisely stated?
- Are the methods described comprehensively?
- Are the interpretations and consclusions justified by the results?
- Are adequate references made to other Works in the field?
- Is the language acceptable?

Reviewers must ensure that all the information related to submitted manuscripts is kept as confidential and must report to the editor if they are aware of copyright infringement and plagiarism on the author's side.

A reviewer who feels unqualified to review the topic of a manuscript or knows that its prompt review will be impossible should notify the editor and excuse himself from the review process.

The editor informs the reviewers that the manuscripts are confidential information and that this is a privileged interaction. The reviewers and editorial board cannot discuss the manuscripts with other persons. The anonymity of the referees is important.

Plagiarism Policy

All submissions are screened using similarity detection software at least two times: on submission and after completing revisions. In the event of alleged or suspected research misconduct, e.g., plagiarism, citation manipulation, or data falsification/fabrication, the editorial board will follow and act in accordance with COPE guidelines. Plagiarism, including self-plagiarism, that is identified at any stage will result in rejection of the manuscript.

Publication Charges Policy

The Clean Energy Technologies Journal assesses no submission fees, publication fees, or page charges.

Retraction Policy

The publisher will take all appropriate measures to modify the article in question, in close cooperation with the editors, in cases of alleged or proven scientific misconduct, fraudulent publication, or plagiarism. This includes the prompt publication of an erratum, disclosure, or retraction of the affected work in the most severe case.

Together with the editors, the publisher will take reasonable steps to detect and prevent the publication of articles in which research misconduct occurs and will under no circumstances promote or knowingly allow such abuse to occur.

Withdrawal Policy

The Clean Energy Technologies Journal is committed to providing high quality articles and uphold the publication ethics to advance the intellectual agenda of science. We expect our authors to comply with, best practice in publication ethics as well as in quality of their articles.

Withdrawal of a manuscript will be permitted only for the most compelling and unavoidable reasons. For withdrawal of a manuscript authors need to submit an "Article withdrawal Form", signed by all authors mentioning the reason for withdrawal to the Editorial Office. Authors must not assume that their manuscript has been withdrawn until they have received appropriate notification to this effect from the editorial office.

In a case where a manuscript has taken more than five months' time for review process, that allows the author to withdraw manuscript.

Manuscript withdrawal penalty: After receiving the Article withdrawal Form, the Clean Energy Technologies Journal Editorial Board will investigate the reason of withdrawal.

If the reason finds to be acceptable, the author is allowed to withdraw the manuscript without any withdrawal penalty. If not the Clean Energy Technologies Journal will not accept any manuscripts from the same author for one year.

Important notes: Manuscripts may be withdrawn at any stage of review and publication process by submitting a request to the editorial office. Manuscript withdrawal will be permitted after submission only for the most compelling and unavoidable reasons.

If the author wants to withdraw a manuscript, the author needs to submit a completed "Article withdrawal Form", signed by all authors of the manuscript stating the reasons for manuscript withdrawal.

The manuscript will not be withdrawn from publication process until a completed, signed form is received by the editorial office. Authors must not assume that their manuscript has been withdrawn until they have received appropriate notification to this effect from the Clean Energy Technologies Journal editorial office.

CLEAN ENERGY TECHNOLOGIES JOURNAL

CONTENTS

Research Article

Post-disaster EV dispatch for powering base stations: A MILP approach to maximize spatiotemporal coverage

Ramazan KILIÇ[1*] , Alper Kağan CANDAN[2] , Ali Rıfat BOYNUEĞRİ[3]

¹Department of Energy Technologies, Yildiz Technical University, Istanbul, Türkiye
²Department of Electrical and Electronics Engineering, Manisa Celal Bayar University, Manisa, Türkiye
³Department of Electrical Engineering, Yildiz Technical University, Istanbul, Türkiye

ABSTRACT

Disasters frequently disable the electrical grid, jeopardizing communication infrastructure and causing severe disruptions in emergency communications. Ensuring rapid deployment of power sources for base stations (BSs) is therefore critical in post-disaster conditions. This study presents a mixed-integer linear programming (MILP) framework that dispatches a fleet of electric vehicles (EVs) to energize multiple BSs and maximizes population-based temporal communication coverage (people × time). In a case study involving 20 BSs and 10 EVs, the optimization prioritizes early service to densely populated areas and delivers a total of 17,597 people for 228 minutes of communication access. Although the served population gradually declines as the energy of the EV fleet depletes, the connectivity is sustained until 16:34. Results demonstrate that feasible EV–BS assignments and service durations are obtained considering BS power demand, coverage areas, and EV initial energy parameters. The proposed model enables communication availability after disasters without relying on additional fixed power resources.

Cite this article as: Kılıç R, Candan AK, Boynueğri AR. Post-disaster EV dispatch for powering base stations: a MILP approach to maximize spatiotemporal coverage. Clean Energy Technol J 2025;3(2):39–49.

INTRODUCTION

In recent years, natural hazards, particularly earthquakes and floods, have increasingly threatened critical infrastructure systems. Power outages following such events trigger cascading service disruptions, severely interrupting daily life. Among the most rapidly affected are communication networks, whose continuity is indispensable during post-disaster response and recovery [1]. The earthquake centered in Kahramanmaraş, Türkiye, starkly revealed this vulnerability: of the 8,900 cellular base stations (BSs) across the ten affected provinces, 2,451 (28%) became non-operational. Although more than 400 mobile BSs with satellite backhaul were deployed, their operation relied on diesel generators (DGs) capable of providing only 3–4 hours of autonomy. Repeated service interruptions occurred due to severe fuel-logistics constraints [2,3]. Ensuring a stable power supply for BSs, the backbone of cellular communi-

*Corresponding author
*E-mail adress: ramazan.kilic@std.yildiz.edu.tr

cation networks, therefore becomes a major challenge under disaster conditions. Traditional power sources are often inaccessible or insufficient, highlighting the need for flexible and rapidly deployable alternatives. Previous research has explored hybrid architectures. Rahman et al. [4] proposed a resilient hybrid energy system (RHES) integrating photovoltaic (PV) generation, proton exchange membrane (PEM) fuel cells, and battery energy storage coordinated through an intelligent energy management system (EMS). The RHES was designed to autonomously supply Base Transceiver Stations (BTS) in grid-independent emergency scenarios. Simulation results demonstrated that BTS operability could be sustained even during prolonged outages, thereby maintaining reliable communication services. Similarly, Ünal and Dağteke [1] developed PV fuel cell hybrid systems capable of providing uninterrupted renewable power to BS following disasters. In addition, Okundamiya et al. conducted a comprehensive assessment of renewable-energy-based hybrid power systems for mobile telecommunication sites, demonstrating that PV–wind–battery configurations can significantly reduce operational costs and enhance BS power reliability in regions with unstable grid access[5]. In a comprehensive survey, Cabrera-Tobar et al. emphasized the vulnerability of telecommunication infrastructure, particularly BSs, to power interruptions stemming both from technical failures and climate-induced hazards. To mitigate these risks, the authors examined a broad set of resilience strategies structured around the phases of preparedness, response, and recovery, including mobile DGs, electric vehicle (EVs) fleets, energy storage systems (ESSs), and stand-alone microgrids (MGs) [6]. Rudenko et al. [7] similarly highlighted that replacing DGs used for mobile BSs with hybrid systems combining hydrogen fuel cells, solar power, and wind energy can ensure reliable off-grid operation while reducing environmental impacts. Such hybrid configurations play a key role in enhancing the sustainability and resilience of telecommunication systems.

Motivated by the growing need for rapidly deployable power solutions for communication systems in post-disaster conditions, this study proposes an optimization-based framework for supplying energy to BS using EVs. The model jointly determines the allocation and scheduling of multiple EVs, each with a distinct initial state of energy (SOE), to BS that differ in power requirements and coverage areas [8]. The objective is to identify the most effective EV–BS matching by maximizing a population–temporal accessibility metric, defined as the product of the number of communications served people and the duration of service provision. The primary contributions of this work are summarized as follows.

A post-disaster EV fleet management framework designed to sustain and extend the operational availability of cellular communication services by supplying emergency power to BS.

Highlights

- MILP model optimizes EV dispatch and BS activation under energy limits
- Cell-based population metrics maximize spatiotemporal coverage.
- Framework extends BS operation without fixed power infrastructure.

A rigorous optimization model that, under EV energy and mobility constraints, determines optimal EV–BS allocation strategies to maximize population-temporal accessibility during disaster-induced grid outages.

The remainder of this article is organized as follows. Section 2 (*Methodology*) describes the overall system model, outlines the modeling assumptions, and formally states the problem. This section also elaborates on the population–time accessibility metric, together with the decision variables and the full set of optimization constraints. Section 3 (*Results*) presents the case study configuration, parameterization, and numerical results derived from the proposed framework. Finally, Section 4 (*Conclusions*) provides a comprehensive synthesis of the findings, interprets the implications of the results for post-disaster communication resilience, and highlights promising avenues for future research.

MATERIALS AND METHODS

This study examines a post-disaster scenario in which cellular BS are subjected to a prolonged grid outage and an EV fleet is deployed as a mobile power supply resource. Each BS is characterized by a fixed power demand and an associated population density within its coverage area, while each EV is defined by its initial SOE and maximum power delivery capability. Since the number of BSs exceeds the number of available EVs, only a limited subset of BSs can be energized at any given time. Moreover, heterogeneous BS types possess different coverage capabilities and consequently differ in the number of users they can serve. Under these conditions, the system operator must determine, over a finite planning horizon, which BS will be energized by each EV while considering the activation duration of each EV–BS assignment. To address this decision-making problem, an EV dispatch strategy is formulated as a mixed-integer linear programming (MILP) optimization model.

EV–BS Spatial Configuration and Distance Computation

The primary objective of the proposed optimization algorithm is to maximize the cumulative population–time accessibility (people × time) by ensuring the continuous energization of BS throughout the disruption horizon following a disaster. Let the discrete time domain be represented by
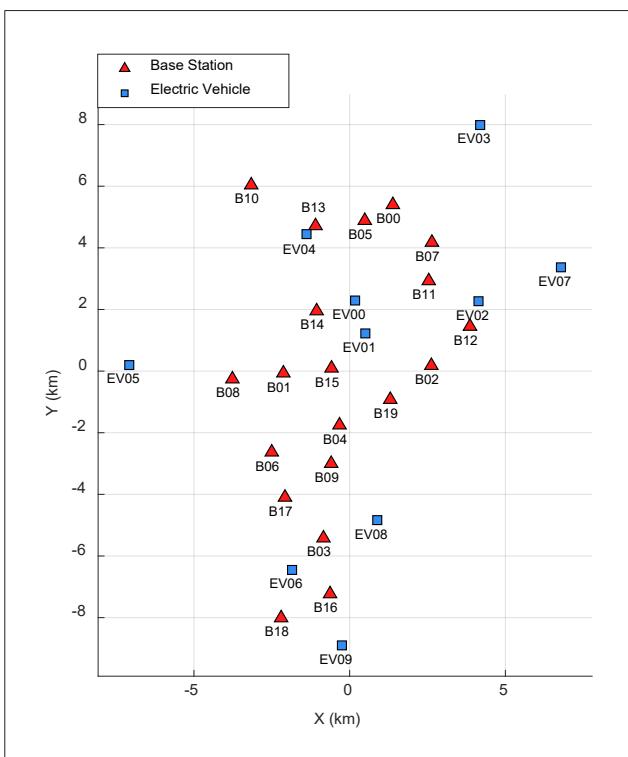
Figure 1. Cartesian coordinates of EV and BS.

$t \in T$, the set of BSs by $b \in B$, and the set of EVs, utilized as mobile power sources, by $e \in E$. Prior to the disaster event, the spatial positions of the EV fleet are defined in a Cartesian coordinate system as $X_e^{EV} \in \mathbb{R}^2$ (1), while the geographical locations of the BS are similarly represented as $X_b^{BS} \in \mathbb{R}^2$ (2), as illustrated in Figure 1. Based on these spatial representations, the Euclidean distance between each EV and each BS at the initial time step $t = 0$ is denoted by $\beta_{e,b}$ (3). Using this rate, the total travel energy required for EV e to reach BS b is computed as $E_{e,b}^{\text{travel}}$ (4). These definitions collectively establish the fundamental spatial and energetic relationships governing the EV–BS assignments within the proposed optimization framework.

$$X_e^{EV} = (x_e^{EV}, y_e^{EV}) \in R^2 \qquad (1)$$

$$X_b^{BS} = (x_b^{BS}, y_b^{BS}) \in R^2 \qquad (2)$$

$$\beta_{[e,b]} = \sqrt[2]{(x_e^{EV} - x_b^{BS})^2 + (y_e^{EV} - y_b^{BS})^2}[km] \qquad (3)$$

$$E_{e,b}^{travel} = \gamma \cdot \beta_{[e,b]} \quad [watt.min] \qquad (4)$$

Once an EV arrives at its determined BS, it immediately initiates the power supply. The corresponding travel time required for EV e to reach BS b is formally denoted as $t_{\text{arr}(e,b)}$ (5).

$$t_{arr[e,b]} = \left\lceil \frac{\beta_{[e,b]}}{v_{ev}} \right\rceil [min] \qquad (5)$$

$$\Delta_{[t,e,b]} = 1 \begin{cases} 1, & t = t_{arr[e,b]} \\ 0, & otherwise \end{cases} \qquad (6)$$

The variable $\Delta_{t,e,b}$ (6) is defined as a binary indicator specifying whether EV e has arrived at BS b at time t. The indicator takes the value $\Delta_{t,e,b} = 1$ when the EV reaches the corresponding BS, and $\Delta_{t,e,b} = 0$ otherwise. For each EV–BS pair, the arrival event can occur at most once; therefore, $\Delta_{t,e,b} = 1$ may be assigned at exactly one time step for every (e, b) pair (7).

$$\sum_{t=1}^{AS-1} \Delta_{[t,e,b]} = 1 \qquad (7)$$

Coverage Cells and Population Density

The computation of cumulative population–time communication access and population density in this study is carried out over a cell-based grid system. The two-dimensional grid is constructed using a uniform coordinate structure defined along the X and Y axes, with each grid cell represented by its centroid, denoted as $X_i = (x_i, y_i)$. The grid dimensions are given by $|X| \times |Y|$, and the total number of cells is denoted by C. Each grid cell has a side length of D [km], and its area is defined as $A_{\text{cell}} = PCA = D^2 [km^2]$.

For each BS $b \in B = \{1, \dots, B\}$, a coordinate vector X_b^{BS} (2) and a coverage radius r_b are defined. Using these parameters, a coverage matrix $S_{b,c} \in \{0,1\}^{B \times C}$ is constructed for all grid cells. The matrix entry $S_{b,c} = 1$ if cell c lies within the coverage area of BS b, and $S_{b,c} = 0$ otherwise. In addition, a binary variable $N_{b,c}$ (8) is introduced to indicate whether cell c is covered by at least one BS.

$$N_{b,c} = 1 \left\{ \sum_{b \in B} S_{b,c} > 0 \right\} \qquad (8)$$

To spatially represent post-disaster population density within the model, macro-circles (macro coverage areas) are defined. For each macro-circle $m \in M$, the center coordinates $c_m = (x_m, y_m)$, the radius R_m, the central population density $\rho_m^{(center)}$, and the edge population density $\rho_m^{(edge)}$ are specified. The Euclidean distance between the center of macro-circle m and the center of grid cell c is computed by $d_m(i)$, as given in Equation (9).

$$d_m(i) = \sqrt{\sum_{j=1}^{p} (x_{i,j} - c_{m,j})^2} \qquad (9)$$

If the $d_m(i) \leq R_m$, the cell is considered within the coverage area of macro-circle m. In this case, the population density assigned to the cell is computed as $\rho_m(i)$ (10) Inside the macro-circle $d_m(i) \leq R_m$.

$$\rho_m(i) = \rho_m^{edge} + \left(\rho_m^{center} - \rho_m^{edge}\right)$$

$$\left(1 - \frac{d_m(i)}{R_m}\right) \tag{10}$$

Not contained within macro-circle m, where $d_m(i) > R_m$:

$$\rho_m(i) = 0 \tag{11}$$

A linear decay function is defined for the macro-circle population density such that the density attains its maximum value at the macro-circle center and decreases to a minimum at the outermost cells. If a cell lies beyond the macro-circle, its population density is assigned as $\rho_m(i) = 0$ (11). Since a cell may fall within the coverage areas of multiple macro-circles, the final macro-circle population density is determined as $\rho_{max}(i)$ (12) which corresponds to the maximum value among all macro-circles for that cell.

$$\rho_{max}(i) = \underset{m}{max}\,\rho_m(i) \tag{12}$$

Finally, the overall population density for each cell is defined as ρ_c. If the cell lies within macro-circles, its value is assigned as $\rho_c = \rho_{max}(i)$. For cells outside the macro-circles, the density is determined based on their coverage status, ensuring a seamless transition between high-density macro regions and the surrounding settlement area. In this manner, a continuous, cell-based pop-
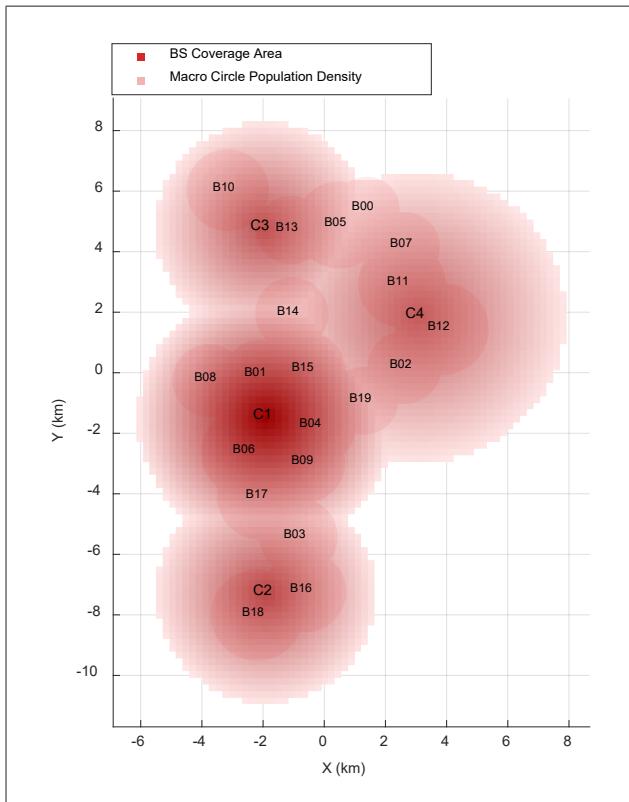
Figure 2. Coverage areas of the BSs and the population density distribution.

ulation density function is established across the entire study region.

Through this formulation, the population density can be represented on the grid plane as a parametric and computationally tractable function, allowing coverage maps to be directly integrated into the optimization model. In post-disaster scenarios in particular, these macro regions correspond to critical settlement areas. Figure 2. presents the resulting population density map, which includes both the macro regions and the coverage areas of the BSs.

Energy and EV–Base Station Matching

The total amount of energy that can be supplied to all BSs is constrained by the initial SOE of the EV fleet (13).

$$PS_{max} = \sum_{e=1}^{E} SOE_e^{\text{init}}\,[Watt.min] \tag{13}$$

At the beginning of the disaster response, each EV is required to be assigned to a single BS. To represent this allocation, the binary variable $B_{e,b}^{EV,L}$ is introduced, indicating whether

EV e is assigned to BS b. This formulation ensures that every EV is allocated to only one BS.

$$\sum_{b=1}^{B} B_{e,b}^{EV,L} = 1 \tag{14}$$

In addition, to ensure that each BS can receive at most one EV:

$$\sum_{e=1}^{E} B_{e,b}^{EV,L} \leq 1 \tag{15}$$

The EV–BS assignment is modeled as a one-to-one matching. This structure prevents any vehicle from being assigned to multiple BSs simultaneously and likewise ensures that no more than one vehicle is located at a given BS. As a result, the distribution of energy across BSs becomes balanced and operationally manageable.

This equality expresses, in a time-traceable manner, the BS to which each EV is assigned. For this purpose, a continuous index variable $EV_{t,e}$ (16) is defined. The BS assignment determined for each EV at the beginning of the disaster remains fixed throughout the entire time horizon; this requirement is enforced by the following equality:

$$EV_{[t,e]} = \sum_{b=0}^{TBSN-1} b \cdot B_{e,b}^{EV,L} \tag{16}$$

Base Station Energy Balance

The time-dependent SOE for each BS is denoted by $\text{SOE}_{(t,b)}^{BS}$ (19). This SOE level is updated through an energy-balance equation that incorporates the previous SOE $\text{SOE}_{(t-1,b)}^{BS}$, the energy

consumed during the preceding time step $P_{(t-1,b)}^{(BS,A)}$, and the net amount of energy delivered by an EV upon arrival $SOE_{(t,b)}^{arr}$ (17). In this statement, SOE_e^{init} denotes the initial energy available in EV e, while $E_{(e,b)}^{travel}$ represents the amount of energy the vehicle must expend to reach BS b. Prior to the beginning of the disaster, the initial SOE of all BSs is assumed to be zero, i.e., $SOE_{(0,b)}^{BS} = 0$ (18).

$$SOE_{t,b}^{arr} = \sum_{e=0}^{TEVN-1} B_{e,b}^{EV,L} . (SOE_e^{init} - E_{e,b}^{travel}) . \Delta_{t,e,b} \tag{17}$$

$$SOE_{0,b}^{BS} = 0 \tag{18}$$

$$SOE_{t,b}^{BS} = SOE_{t-1,b}^{BS} - P_{t-1,b}^{BS,A} + SOE_{t,b}^{arr} \tag{19}$$

The inequality $SOE_{(0,b)}^{BS}$ (20) stabilizes the initial state of the system, ensuring a consistent progression of the time series. Moreover, this requirement prevents the SOE variable from ever taking negative values, thereby preserving the physical validity of the model.

$$SOE_{0,b}^{BS} \geq 0 \tag{20}$$

To enable EV to supply power to BS, each vehicle must possess a sufficient amount of battery energy to reach the corresponding BS. Accordingly, for every EV $e \in E$ and every BS $b \in B$, an accessibility binary variable $REACH_{e,b}$ (21) is introduced. This variable is determined by comparing the initial SOE of the EV with the travel energy required to reach BS b. A value of $REACH_{e,b} = 1$ indicates that EV has adequate energy to reach the BS, whereas $REACH_{e,b} = 0$ signifies that it does not.

$$REACH_{e,b} = \begin{cases} 1, & if \quad SOE_e^{init} \geq E_{e,b}^{travel} \\ 0, & otherwise \end{cases} \tag{21}$$

Based on these definitions, an EV can only be assigned to BSs that are energetically reachable, i.e., BSs for which the required travel energy does not exceed the vehicle's initial energy. Accordingly, the assignment variables $B_{(e,b)}^{(EV,L)}$ are restricted by this accessibility mask, which is formally expressed in (22).

$$B_{e,b}^{EV,L} \leq REACH_{e,b} \tag{22}$$

If $REACH_{e,b} = 0$, the assignment of EV e to BS b becomes mathematically infeasible; consequently, any physically unreachable assignment combinations are automatically excluded from the model. For each BS, the power consumed when the BS is active $P_{t,b}^{(BS,A)}$ (23), is expressed directly in terms of its nominal power capacity. This relationship is defined by the following equality:

$$P_{t,b}^{BS,A} = P_b^c . U_{t,b} \tag{23}$$

This equality expresses $P_{t,b}^{(BS,A)}$ as the power consumption of BS b at time t. The term P_b^c denotes the nominal power capacity of the BS, while $U_{t,b}$ (24) is a binary decision variable indicating whether the BS is active at that specific time step. When $U_{t,b} = 1$, the BS is operational and draws its nominal power; when $U_{t,b} = 0$, the BS is inactive and its power consumption becomes zero.

$$U_{t,b} \in \{0,1\} \tag{24}$$

The SOE of BS b at time t, expressed as $SOE_{t,b}^{BS}$ (25), represents the total amount of energy stored at that BS. This quantity is constrained to remain non-negative at all times.

$$SOE_{t,b}^{BS} \geq 0 \tag{25}$$

A BS can be activated only if its SOE exceeds a predefined minimum operational threshold. This operational condition (26) is formulated as follows.

$$SOE_{t,b}^{BS} \geq SOE_e^{min} . U_{t,b} \tag{26}$$

When $U_{t,b} = 1$, BS b can be activated at time t; when, $U_{t,b} = 0$ BS b cannot be activated at time t. At the beginning of the post-disaster (i.e., t=0), all BS are assumed to be inactive (27). This assumption implies that no energy supply or EV deployment is available at the moment the disaster occurs. Consequently, it removes any ambiguity regarding the initial SOE of the BS and the timing of the first activation.

$$U_{0,b} = 0 \tag{27}$$

At each time step, the number of BSs that can be activated is physically limited by the number of available EV, since activating any BS requires at least one energy source. This constraint (28) is formulated as follows.

$$\sum_{b=0}^{TBSN-1} U_{t,b} \leq TEVN \tag{28}$$

With this approach, an upper bound is imposed on multiple BSs are activated that can be simultaneously active at any given time step. This constraint enhances the consistency of the model with real-world operational conditions and prevents physically infeasible scenarios involving unlimited BS activations. On the other hand, for a BS to become active, there must be at least one EV at its location. As mentioned earlier, activation is not possible in any location where there is no EV. This relationship is expressed as follows.

$$U_{t,b} \leq \sum_{e=0}^{TEVN-1} B_{e,b}^{EV,L} \tag{29}$$

As previously stated, the binary decision variable $B_{e,b}^{EV,L}$ indicates whether EV e is located at BS b. If no EV is assigned to BS b, the right-hand side of the constraint becomes zero, implying $U_{t,b} = 0$. A BS can be activated only if exactly one EV is located at that position and sufficient SOE is available.

Conversely, there is no activation at any BS where no EV is present, ensuring that $U_{t,b} \leq 1$.

The activation of a BS b is not solely contingent upon an EV e being assigned to that BS but also requires that the EV physically arrives there within a specific time step t. For this reason, BS activation is formulated with explicit consideration of EV arrival times. As previously introduced, the arrival indicator $\Delta_{t,e,b}$ (8) captures this temporal condition. Considering these conditions, an arrival matrix $A_{t,e,b}^{\text{arr}}$ (30) is defined to indicate whether an EV remains present at a BS b during all time steps following its arrival. This matrix captures the temporal persistence of an EV at BS after it reaches the location.

$$A_{t,e,b}^{\text{arr}} = 1\left(\sum_{\tau=1}^{t} \Delta_{[\tau,e,b]} > 0\right) \tag{30}$$

This expression indicates whether the EV has arrived at the BS at some time $\tau \leq t$. Accordingly, the indicator $A_{t,e,b}^{\text{arr}}$ takes the value 1 for all time steps following the arrival of EV e at BS b. The activation of a BS is formalized through the product of the assignment variable and the arrival matrix. This relationship (31) is expressed formally by the following equality.

$$U_{t,b} \leq \sum_{e \in E} B_{e,b}^{EV,L} \cdot A_{t,e,b}^{arr} \tag{31}$$

The capability of a BS to be activated precisely at the moment of an EV's arrival is represented by the variable $U_{t,b}^{\text{can}}$ (32). This binary decision variable, $U_{t,b}^{\text{can}} \in \{0,1\}$, takes the value 1 only at the exact time step when the EV reaches BS b, and remains 0 at all other times.

$$U_{t,b}^{can} = \sum_{e=0}^{TEVN-1} B_{e,b}^{EV,L} \cdot \Delta_{t,e,b} \tag{32}$$

The variable $U_{t,b}^{\text{can}}$ functions as a binary triggering mechanism within the decision structure of the model. When an EV arrives at its corresponding BS, this variable enables the initiation of activation at time t. If an EV is both assigned to that BS and reaches it at the exact arrival time, then $U_{t,b}^{\text{can}} = 1$, thereby allowing the BS to be activated. In summary, $U_{t,b}^{\text{can}}$ is an internal model variable that triggers a specific decision mechanism. In contrast, $\Delta_{t,e,b}$ is a pre-computed indicator determined by parameters such as travel distance, average speed, and departure time. With respect to the energy threshold, the arrival of an EV alone is not sufficient for activating a BS at the moment of arrival; the minimum required energy level must also be satisfied. This condition is formally imposed by constraint (33).

$$(SOE_{t-1,\,b}^{BS} + SOE_{t,b}^{arr}) \geq (SOE_e^{min}) \cdot U_{t,b}^{can} \tag{33}$$

When this energy threshold is satisfied, the activation of the BS becomes appropriate and is mandatorily triggered (34). However, if the required energy level is not available,

the BS remains inactive even if $U_{t,b}^{\text{can}} = 1$; in such cases, the energy-threshold constraint prevents activation.

$$U_{t,b} \geq U_{t,b}^{can} \tag{34}$$

Base Station Deactivation Condition

The activation status of each BS at time is represented by the binary decision variable $U_{t,b} \in \{0,1\}$, as previously defined. A transition of a BS from the active state to the inactive state (i.e., $1 \rightarrow 0$) is classified as a *deactivation event*. To capture this event, a binary indicator $U_{t,b}^{off} \in \{0,1\}$(35) is utilized. The detection of a deactivation event is formally defined by the following linear inequality:

$$U_{t,b}^{off} \geq U_{t-1,b} - U_{t,b} \tag{35}$$

Considering this shutdown indicator, inequality (36) provides a consistent criterion for determining the physical conditions under which a BS can transition from an active state to a shutdown state. The left-hand side of the inequality,

$$SOE_{t-1,b}^{BS} + SOE_{t,b}^{arr}$$

Represents the total amount of energy effectively available at BS at the beginning of time step t. This total consists of the energy carried over from the previous minute, $SOE_{t-1,b}^{BS}$, and the net arrival energy $SOE_{t\,b}^{arr}$, which is transferred only if an EV reaches the BS precisely at minute t. The arrival energy is zero at all other time steps. The right-hand side of the inequality,

$$SOE_e^{min} + P_b^c$$

Defines the highest permissible energy level at which a shutdown event can be considered physically feasible. This threshold ensures that the BS cannot be switched off as long as it possesses sufficient energy to meet its mandatory safety reserve SOE_e^{min} and its nominal one-minute power demand P_b^c. Therefore, a shutdown is physically meaningful only when

$$SOE_{t-1,b}^{BS} + SOE_{t,b}^{arr} \leq SOE_e^{min} + P_b^c$$

Is satisfied.

The Big-M term,

$$M_b^{off}(1 - U_{t,b}^{off})$$

Ensures that this threshold condition is enforced only when the model attempts to issue a shutdown decision. If $U_{t,b}^{off} = 1$ (i.e., a shutdown is being attempted), the Big-M term vanishes and the inequality becomes binding; in this case, if the total energy exceeds the threshold, constraint (36) would be violated, preventing the model from shutting down the BS. Conversely, if no shutdown is triggered ($U_{t,b}^{off} = 0$), the large value of M_b^{off} relaxes the constraint, avoiding any artificial restriction on the natural evolution of the energy stock and allowing the BS to continue operating normally. Bringing all components together, the shutdown condition is formally expressed as: $SOE_{t-1,b}^{BS} + SOE_{t,b}^{arr}$

$$\leq SOE_e^{min} + P_b^c + M_b^{off}$$
$$(1 - U_{t,b}^{off}) \tag{36}$$

This formulation ensures that BS shutdowns occur only under physically meaningful energy conditions, thereby preserving both the operational realism and the temporal consistency of the model.

Coverage Cells and Total Population

In this section, to enable an accurate assessment of the total covered area and total covered population, the coverage areas of the BSs are considered not only in terms of their geographic locations but also with respect to their mutual overlap relationships. Accordingly, the model defines two fundamental concepts using the cell-based coverage map $S_{b,c}$.

Pattern coverage: refers to regions in which multiple BSs simultaneously cover the same cell.

Single coverage: refers to cells that are covered exclusively by a single BS.

This distinction eliminates potential double-counting issues, ensuring that the population contained within each cell is accounted for exactly once in all calculations. Definition of Cells and Population Density:

- Cell area: $A_{cell} = PCA$ [km²/cell]

- Cell population density: ρ_c[people/cell]

The coverage status of the BSs is represented by the binary matrix $S_{b,c} \in \{0,1\}$. This matrix identifies, for each cell, which BS provide coverage, thereby explicitly characterizing the active coverage relationships across the grid. Subsequently, these two data sets are aggregated within a linear framework by linking them to the time dependent activation status of the BS. The notation used throughout this formulation is as follows: $b \in \{1, ..., B\}$ denotes the set of BSs; $c \in \{1, ..., C\}$ denotes the grid cells; $p \in \{1, ..., P\}$ represents the coverage patterns; and $t \in \{1, ..., T\}$ corresponds to the time steps.

Pattern Coverage

In this study, a pattern is defined as a subset of cells that are simultaneously covered by multiple BS. Each pattern p is represented by a vector indicating which BS contribute to that pattern. The pattern–BS relationship is expressed by the binary parameter $PT_{p,b} \in \{0,1\}$, where $PT_{p\,b} = 1$ denotes that BS b is part of pattern p.

$$PT_{p,b} = \begin{cases} 1 \text{ if BS } b \text{ is part of pattern p} \\ 0 \qquad\qquad\qquad otherwise \end{cases} \tag{37}$$

Coverage Cell and Pattern

The pattern to which a cell belongs is determined by the exact matching between its coverage vector and the corresponding pattern vector.

$$M_{p,c} = \begin{cases} 1, & PT_P = S_c \\ 0, & otherwise \end{cases} \tag{38}$$

In other words, a cell is regarded as belonging to a particular pattern if the set of BSs covering that cell coincides exactly with the BS set defined by that pattern.

Single Coverage

In order to obtain the cell-level coverage structure of the BSs in a detailed manner, the coverage degree deg(c)(39) associated with each cell is first defined. For this purpose, by using the binary coverage matrix $S_{b,c} \in \{0,1\}$ defined over the set B of BSs and the set of C cells (where $S_{b\,c} = 1$ if BS b covers cell c), the coverage degree of each cell is computed as

$$\deg(c) = \sum_{b \in B} S_{b,c}, \quad c \in C \tag{39}$$

The coverage degree deg (c) indicates how many different BSs cover cell c, and it plays a fundamental role in determining the single-coverage condition. Accordingly, in order to distinguish the cells that are covered by only one BS, a cell-based binary singularity indicator (40) is defined as

$$H_c = \begin{cases} 1, & \text{if } \deg(c) = 1, \\ 0, & otherwise, \end{cases} \quad c \in C \tag{40}$$

This indicator mathematically labels the cells under single coverage and enables the separation of multiple-overlap regions within the coverage matrix. To extend the single-coverage structure to the BS–cell dimension, the indicator H_c is multiplied by the coverage matrix, and a new matrix (41) is obtained as

$$G_{b,c} = S_{b,c} H_c, \qquad b \in B, c \in C \tag{41}$$

Thus, $G_{b,c} = 1$ occurs only under the following conditions: (i) cell is under single coverage ($H_c = 1$), and (ii) the only BS covering this cell is b ($S_{b,c} = 1$). Therefore, the matrix $G_{b,c}$ precisely identifies the single-coverage area specific to each BS by automatically separating multi-coverage areas and uncovered cells. Using this structure, the total number of cells in the single-coverage area of BS b is defined as

$$N_b^{sgl} = \sum_c G_{b,c} \tag{42}$$

and it is employed as a quantitative indicator of the single-coverage capacity.

Computation of Average Single-Coverage Population Density

For each BS, the number of cells exclusively covered by that BS was defined earlier. Building on this definition, the total population residing within these single-coverage cells is denoted by R_b^s (Equation 43).

$$R_b^s = \sum_c G_{b,c} \cdot \rho_c \tag{43}$$

By taking the ratio of these quantities, the average population density under single coverage for each BS is obtained as $\bar{\rho}_b^s$ (44).

$$\bar{\rho}_b^s = \frac{R_b^s}{\max(N_b^{sgl})} \tag{44}$$

Computation of Average Pattern-Based Population Density

In this expression, n_p (45) denotes the total number of cells covered by pattern p. Each pattern p represents a structural coverage configuration characterized by its own distinct set of BS.

$$n_p = \sum_c M_{p,c} \tag{45}$$

R_p (46) represents the total population contained within the cells covered by pattern p and is expressed as follows.

$$R_p = \sum_c M_{p,c} \cdot \rho_c \tag{46}$$

In this context, R_p captures the aggregate population contained solely within the cells associated with pattern p. Patterns corresponding to densely populated regions naturally yield larger R_p values, whereas those representing rural or sparsely populated areas exhibit comparatively lower population totals. Consequently, through these two expressions, the average population density for pattern p, denoted by $\bar{p}_p$ (47), is obtained.

$$\bar{p}_p = \frac{R_p}{\max(n_p)} \tag{47}$$

Population and Cell Count Coefficients

α_p: expresses the number of grid cells associated with coverage pattern p, that is, the cells jointly covered by the same combination of BS. Likewise, α_b expresses the number of grid cells that are exclusively covered by BS b, with no overlap from any other BS. Using these parameter values, the total population within the single coverage area of BS b a fixed coefficient is computed as φ_b.

$$\varphi_b = \alpha_b \cdot \bar{\rho}_b^s \tag{48}$$

The total number of people contained within the region corresponding to pattern p, which represents the overlap area, is computed as a fixed coefficient and is expressed as φ_b (49).

$$\varphi_p = \alpha_p \cdot \bar{p}_p \tag{49}$$

Pattern Activation Constraint

For a pattern p to be activated ($Z_{p,t} = 1$), at least one of the BSs constituting that pattern must be active, and this requirement is expressed by inequality (50). If pattern p is not active ($Z_{p,t} = 0$), none of the BSs associated with that pattern is allowed to operate, and this condition is captured by inequality (51).

$U_{t,b} \in \{0,1\}$ BSs activation decision variable

$Z_{p,t} \in \{0,1\}$ Pattern activation variable, whether pattern p is active at time t is determined by its corresponding activation variable.

$$\sum_{b \in B} U_{t,b} \geq Z_{p,t}, \tag{50}$$

$$U_{t,b} \leq Z_{p,t} \tag{51}$$

Total Population Served

At time step t, the total population served is defined as the weighted aggregation of all active coverage patterns and active single-coverage BS regions, where φ_p denotes the population weight of pattern p and φ_b represents the mean population coefficient associated with the single-coverage area of BS b. This relationship is expressed as

$$POP_t = \left(\sum_{p \in P} \varphi_p \cdot Z_{p,t} + \sum_{b \in B} \varphi_b \cdot U_{t,b} \right) [person] \tag{52}$$

Objective Function

The objective is to maximize the total number of people served within the communication coverage area throughout the disaster period. This is formulated as follows in (53).

$$\max \sum_{t=1}^{AS} POP_t \tag{53}$$

This objective function implicitly governs the allocation of energy-supplying EV to BS by steering the optimization process toward configurations that yield the greatest communication reach. In effect, it mathematically determines which subsets of BS should be activated so as to maximize the population maintained under operational coverage throughout the disaster period.

RESULTS

The case study focuses on the district of Antakya, located in the Eastern Mediterranean region of Türkiye and one of the areas most severely affected by the Kahramanmaraş earthquakes of 6 February 2023. The test system consists of 20 BSs serving all mobile network operators in Antakya and 10 EVs that can be deployed as mobile power sources. The initial SOE levels of the EV fleet are provided in Table 1. For operational safety, each EV is assigned a minimum SOE threshold of $SOE_e^{min} = 1000 * 60 [Watt.min]$ (17) (1 kWh), which must be preserved in the battery at all times and cannot be used for powering BSs. For mobility modeling, a constant travel-energy consumption rate of $\gamma = 9000$

Table 1. The initial (SOE) of the EVs.

EVs	Initial SOE (kWh)
1	71
2	66
3	61
4	56
5	51
6	46
7	41
8	36
9	31
10	26

Table 2. Coverage areas and power consumption of BSs.

BS index	BSs coverage area (km²)	BSs power (Watt)
1	3.7	4000
2	4.1	5000
3	4.5	6000
4	5	4500
5	5.7	5500
6	6.6	6500
7	6.9	4200
8	4.1	5200
9	4.5	6200
10	5.1	4800
11	5.7	5800
12	6.4	6800
13	6.9	4100
14	4.1	5100
15	4.7	6100
16	5.1	4300
17	5.8	5300
18	6.4	6300
19	6.9	4900
20	4.1	5900

W·min per kilometer is assumed for all EV, reflecting an average traction demand during displacement. Additionally, the average travel speed of the EVs is modeled as uniform and set to $V_{ev} = 50/60$ km per minute, providing a consistent basis for computing travel times across the network. During the earthquake, 64 of the 67 rooftop BSs in Antakya were destroyed or severely damaged, whereas 32 of the 34 tower-type BSs remained operational [9]. Consistent with these findings, a tower-based configuration representative of urban/suburban deployments has been adopted as the reference model in this study. In the population model used in this case study, cells located outside all macro-circles but within the coverage area of at least one BS are assigned a density of $P_c = 20$ people per cell, while cells lying outside both macro-circles and BS coverage areas are assigned $P_c = 5$ people per cell.

The proposed MILP model was developed in Python and solved using the Gurobi Optimizer (version 11.0.3). All simulations were performed on a computer with an Intel i5-7200U processor and 12 GB of memory. The total solution time for the Antakya case study was approximately 31 minutes.

The power requirements of BS vary on the order of several kilowatts, depending on factors such as radio configuration, transmission power, and site-specific auxiliary loads (e.g., cooling). Capacity-oriented small-cell deployments in higher frequency bands (e.g., 1800–2600 MHz) typically consume up to approximately 1 kW[10] [11], whereas macro sites operating in sub-GHz bands (e.g., 700/800/900 MHz) and providing wide-area coverage may require 5 kW or more when cooling and ancillary systems are included [4][12][13]. Cooling alone often accounts for 25–30% of total site energy consumption[14][15]. For this reason, the study incorporates different BS types. The BS-specific power demands and coverage radii used in the case study are reported in Table 2.

In this model, the EVs begin supplying power to the BSs starting from minute 2. By minute 21, all EVs have reached their assigned BSs and have energized them using their arrival SOE $SOE_{t,b}^{arr}$. At minute 21, the total number of people able to maintain communication reaches its maximum value of 17,597, as demonstrated in Figure 3. This result is reported in Table 3.

The matching between the EV and the BS is provided in Table 3. Based on these assignments, the energy consumed by each EV while traveling to its designated BS is computed,
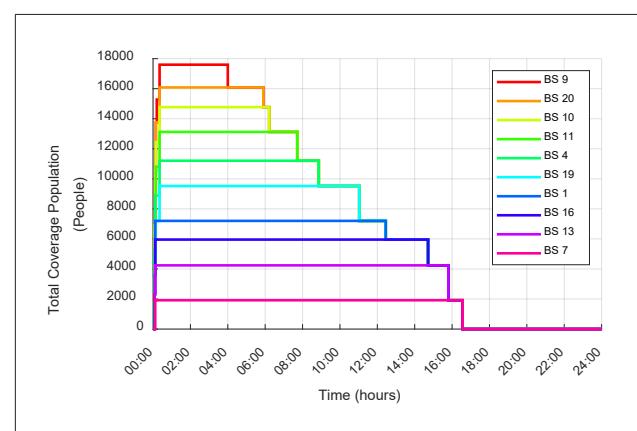
Figure 3. Population covered by bss post-disaster (people).
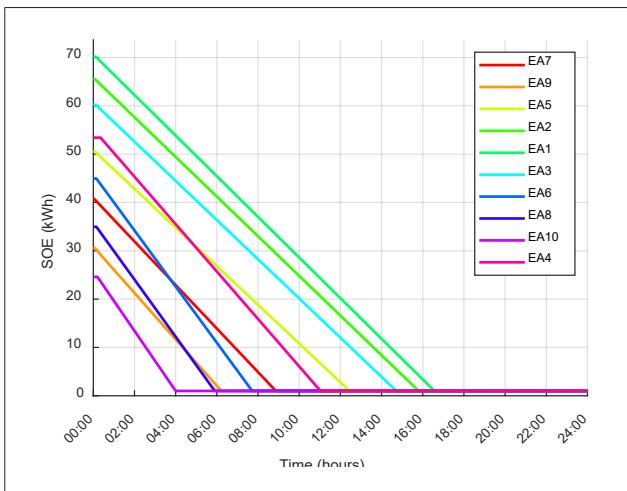
Figure 4. EV SOE at the time of post-disaster BS energization.

Table 3. The energization of BSs by EVs as a function of activation time, and the total number of people able to communicate.

Activation time [Min]	EVs	BSs	Total coverage population [People]
t=2	7	4	1.544
t=3	9	10	3.372
t=4	5	1	4.460
t=5	2	13	6.666
t=7	1	7	10.575
t=7	3	16	10.575
t=9	6	11	14.038
t=9	8	20	14.038
t=12	10	9	15.673
t=21	4	19	17.597

Table 4. EV arrival SOE at BSs and EV–BS distances.

Activation Time [Min]	EVs	BSs	Distance between EVs and BSs [km]	EVs arrival SOE [kWh]
t=2	7	4	1.4	40.78
t=3	9	10	2.4	30.65
t=4	5	1	2.9	50.56
t=5	2	13	3.4	65.49
t=7	1	7	5.6	70.16
t=7	3	16	5.2	60.22
t=9	6	11	7	44.95
t=9	8	20	7	34.96
t=12	10	9	9.3	24.6
t=21	4	19	17.2	53.42

and the resulting arrival SOE $SOE_{t,b}^{arr}$ is determined. These arrival energy values are reported in Table 4. In addition, the minute-by-minute energy consumption of each BS starting from the moment the EV reaches and energizes the site is illustrated in Figure 4.

CONCLUSION

This study develops a MILP framework for dispatching a fleet of EVs to energize BSs during disaster-induced outages, with the objective of maximizing population-based temporal connectivity under energy constraints. In the Antakya case study (20 BS, 10 EV), the optimization yields an extended early-stage service window, maintaining communication access for 17,597 individuals over a period of 228 minutes. As the EVs gradually deplete their energy reserves, the total covered population correspondingly declines, and service ceases at 16:34 local time. These findings demonstrate a viable approach to enable post-disaster communication access without the need for additional fixed generation resources. Moreover, integrating multi-objective planning and hybrid power resources (e.g., fuel-cell EVs, mobile power generators, or battery trucks) could further enhance operational effectiveness. Overall, the model offers a streamlined tool and field-deployable mission plans for emergency managers.

AUTHORSHIP CONTRIBUTIONS

Authors equally contributed to this work.

DATA AVAILABILITY STATEMENT

The authors confirm that the data that support the findings of this study are available within the article. Raw data that support the finding of this study are available from the corresponding author, upon reasonable request.

CONFLICT OF INTEREST

The authors declared no potential conflicts of interest with respect to the research, authorship, and/or publication of this article.

ETHICS

There are no ethical issues with the publication of this manuscript.

REFERENCES

[1]   Unal S, Dagteke SE. Enhancement of fuel cell based energy sustainability for cell on wheels mobile base

stations used in disaster areas. Int J Hydrogen Energy, 2024;75:567–577. [CrossRef]

[2] Kimblad E. Assessing Critical Infrastructure Resilience: a case study of the 2023 Kahramanmaraş earthquakes Holistic Assessment of Critical Infrastructure Resilience during Disasters (HACIRD)-A case study of the 2023 Kahramanmaraş earthquakes. Available at: http://www.risk.lth.se Accessed on Jan 05, 2026

[3] Silva CMMRS, Premadasa PND, Chandima DP, Karunadasa JP, Wheeler P. Optimum sizing and configuration of electrical system for telecommunication base stations with grid power, Li-ion battery bank, diesel generator and solar PV. J Energy Storage 2025;123:116704. [CrossRef]

[4] Rahman MRU, Niknejad P, Barzegaran MR. Resilient Hybrid Energy System (RHES) for Powering Cellular Base Transceiver Station during Natural Disasters. 2021 IEEE Power and Energy Conference at Illinois, *PECI 2021*, Institute of Electrical and Electronics Engineers Inc., 2021. [CrossRef]

[5] Okundamiya MS, Emagbetere JO, Ogujor EA. Assessment of renewable energy technology and a case of sustainable energy in mobile telecommunication sector. Sci World J 2014;2014:947281. [CrossRef]

[6] Cabrera-Tobar A, Grimaccia F, Leva S. Energy resilience in telecommunication networks: A comprehensive review of strategies and challenges. Energies (Basel) 2023;16:6633. [CrossRef]

[7] Curran Associates. 2017 International Conference on Industrial Engineering, Applications and Manufacturing (ICIEAM) : proceedings : South Ural State University (national research university), Chely-abinsk, Russia, May 16-19, 2017. IEEE, 2017.

[8] Ahmed F, Naeem M, Ejaz W, Iqbal M, Anpalagan A, Kim HS. Renewable energy assisted traffic aware cellular base station energy cooperation. Energies (Basel) 2018;11:99. [CrossRef]

[9] Türkiye Bilişim Derneği. Türkiye Bilişim Derneği Türkiye'nin Deprem Gerçeği: Bilişim Çözümleri Deprem ve Bilişim Çalıştayı Raporu Çalıştay Tarihi Raporu. Türkiye Bilişim Derneği. Available at: https://www.tbd.org.tr/en/tbd-deprem-ve-bilisim-calistayi-raporu/ Accessed on Jan 05, 2026.

[10] Deevela NR, Kandpal TC, Singh B. A review of renewable energy based power supply options for telecom towers. Environ Dev Sustain 2024;26:2897–2964. [CrossRef]

[11] Gandotra P, Jha RK, Jain S. Green communication in next generation cellular networks: A survey. IEEE Access 2017;5:11727–11758. [CrossRef]

[12] Lorincz J, Garma T, Petrovic G. Measurements and modelling of base station power consumption under real traffic loads. Sensors 2012;12:4281–4310. [CrossRef]

[13] Kusakana K, Vermaak HJ. Hybrid renewable power systems for mobile telephony base stations in developing countries. Renew Energy 2013;51:419–425. [CrossRef]

[14] Yeshalem MT, Khan B. Design of an off-grid hybrid PV/wind power system for remote mobile base station: A case study. AIMS Energy 2017;5:96–112. [CrossRef]

[15] Rahman M. Overview of energy saving aspects in 2G and 3G Mobile Communication Networks (Master thesis). Swedish: University of Gävle; 2009.

Review Article

CCUS Integration in hydrogen production: Technological advances, sectoral applications, and future perspective

İbrahim ÇAKICI[1] , **E. Ensar SAKARYA[2]** , **Hibat Allah KAZEM[3]** , **Kübra AL[1,4*]** ,
Ender ATEŞ[1] , **Kadir AKGÜN[2]**

[1]Clean Energy Technologies Institute, Yildiz Technical University, Istanbul, Türkiye
[2]Department of Environmental Engineering, Yildiz Technical University, Istanbul, Türkiye
[3]Department of Chemical Engineering, Yildiz Technical University, Istanbul, Türkiye
[4]Department of Energy Systems Engineering, Yalova University, Yalova, Türkiye

ABSTRACT

The integration of carbon capture, utilization and storage (CCUS) technologies into hydrogen production is gaining prominence as a transitional solution to reduce emissions in the energy sector. This study explores the technical, environmental, and economic dimensions of blue hydrogen production, which is based on natural gas reforming methods such as steam methane reforming (SMR) and autothermal reforming (ATR) combined with CCUS. While grey hydrogen has a high carbon footprint, blue hydrogen significantly lowers emissions, achieving reductions of up to 90% depending on carbon capture efficiency. The research also compares various CCUS technologies including post-combustion, pre-combustion, and oxy-fuel combustion, alongside emerging alternatives like membrane separation and chemical looping. A techno-economic analysis highlights the trade-offs between capture efficiency, energy demand, cost, and scalability. Global and national hydrogen strategies, including Türkiye's National Hydrogen Strategy, are examined in terms of CCUS integration potential. The study concludes that although challenges such as infrastructure, cost, and policy remain, CCUS-enabled blue hydrogen plays a significant role in the global energy transition toward net-zero targets.

Cite this article as: Çakıcı İ, Sakarya EE, Kazem HA, Al K, Ateş E, Akgün K. The role of hydrogen in sustainable transportation: An international review of distribution and supply systems. Clean Energy Technol J 2025;3(2):50–61.

***Corresponding author**
*E-mail adress: kubra.al@outlook.com

INTRODUCTION

One of the most important global decisions to prevent climate change is the Paris Agreement and the European Green Deal. These agreements make it necessary to reduce carbon in the energy sector. Today, energy production causes about 73% of global greenhouse gas emissions [1]. This makes the energy sector one of the main reasons for the climate crisis. In this context, hydrogen becomes important because it is a flexible energy carrier and can be produced in different ways [2]. Hydrogen is categorized based on the carbon intensity of its production process. Grey hydrogen is produced from fossil fuels, primarily natural gas, through SMR without any carbon mitigation. Blue hydrogen follows a similar pathway but incorporates CCUS technologies to significantly reduce associated emissions. In contrast, green hydrogen is generated via water electrolysis using renewable electricity, resulting in minimal environmental impact. These classifications reflect the varying environmental performance of hydrogen technologies and emphasize the need for a shift towards low-carbon and renewable options in line with global decarbonization goals. These types show that hydrogen can have very different environmental effects, depending on how it is made. Today, about 95% of hydrogen is produced as grey hydrogen, which uses natural gas with SMR [3]. This method produces about 9–12 tons of CO_2 for every 1 ton of hydrogen [4]. This makes grey hydrogen have a large carbon footprint. Therefore, it is not a clean energy source. To solve this problem, a better method called blue hydrogen is developed. Blue hydrogen uses the same SMR method, but it also includes CCUS technologies. In this way, the CO_2 created during production is either stored underground or used in industry [5]. According to Roy et al. (2025), blue hydrogen can reduce the carbon footprint by 56% to 90%. This means blue hydrogen emits about 3.46 to 8.12 kg CO_2eq per kg of hydrogen [6].

These differences are shown in Figure 1. The figure compares the carbon emissions and capture levels of different types of hydrogen. Grey hydrogen shows the highest emissions, while blue hydrogen shows big improvements depending on the capture rate. Some systems like pale blue hydrogen or floating PV-supported hydrogen even have negative emissions [6].

In another study, Zhang et al.[7] examined the technical and economic development of large-scale blue hydrogen production. They showed that methods like ATR and SMR can reduce total emissions when combined with carbon capture. They also said that efficiency, production scale, and carbon pricing are important for making blue hydrogen more competitive in the market. Today, many large blue hydrogen projects are being developed. For example, the Quest Carbon Capture and Storage Project in Canada captures 1 million tons of CO_2 every year and stores it underground [8]. Also, a report by Honeywell and Topsoe (2024)

Highlights

- Blue hydrogen, when integrated with CCUS, offers up to 90% reduction in CO_2 emissions compared to grey hydrogen.
- Post-combustion, pre-combustion, and oxy-fuel combustion are evaluated as core CCUS technologies for hydrogen production.
- Techno-economic analysis identifies oxy-fuel combustion as the most balanced CCUS method for large-scale industrial applications.
- SMR and advanced catalysts enhance efficiency and carbon reduction in blue hydrogen pathways.
- Türkiye's hydrogen strategy highlights blue hydrogen as a transitional bridge to green hydrogen by 2035.
- Global investment trends and policy tools like carbon pricing and CCfDs are accelerating CCUS deployment in hydrogen sectors.

shows that SynCOR™ ATR technology and cryogenic CO_2 separation can produce hydrogen efficiently with low carbon [9]. Khan et al. [10] made a review about blue hydrogen production from natural gas. They said that blue hydrogen is a low-carbon energy solution. Their study explained that the efficiency of carbon capture, methane leaks, and infrastructure planning are all very important. They also showed how regional differences and government support affect the success of these projects.

On the other hand, Howarth and Jacobson [11] say that methane leaks during natural gas production and transport may reduce the benefits of blue hydrogen. Because of this, we must carefully manage carbon capture systems, underground storage, and the natural gas supply chain. Also, according to the International Energy Agency (IEA-2023),
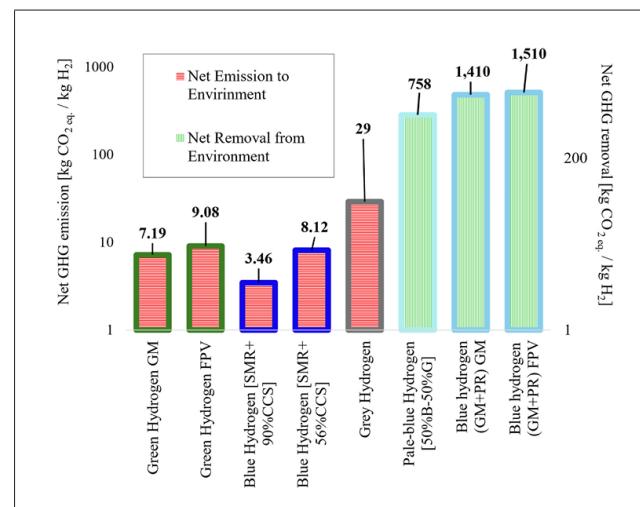

Figure 1. Comparison of Carbon Emissions and Capture Rates of Hydrogen Production Methods [6].

the world plans to reach 40 million tons of blue hydrogen per year by 2030. This can reduce global CO_2 emissions by about 400 million tons [1]. Countries like the European Union (EU), United States of America (USA), and Japan see blue hydrogen as a priority for energy security and low-carbon industry. For example, Germany wants to build 10 Gigawatt (GW) of electrolysis capacity and grow its blue hydrogen sector by 2030 [3]. In Türkiye, the National Hydrogen Strategy (2023) says that by 2035, 70% of hydrogen will be green. But during the transition period, using natural gas infrastructure and CCUS technologies makes blue hydrogen very important [12].

This study focuses on blue hydrogen as a key solution to reduce carbon in energy systems. It will evaluate the technical, economical and environmental results of CCUS technologies in blue hydrogen. The study will also examine how Türkiye and the world can use blue hydrogen in their energy transition policies. Different scenarios will be used to show the emission reduction potential of blue hydrogen. The goal is to give strategic suggestions for global and local energy change.

CCUS TECHNOLOGIES USED IN HYDROGEN PRODUCTION

CCUS technologies primarily entail capturing the emissions of carbon dioxide (CO_2) from industrial processes and fuel combustion, utilizing captured CO_2 for some industrial purposes and then storing the remainder underground securely. The primary technologies for carbon capture are post-combustion, pre-combustion, and oxy-fuel combustion technologies with variations in advantages as well as limitations [13,14].

Post-Combustion Capture

Post-combustion capture captures CO_2 from the flue gases subsequent to the combustion of fossil fuels. It prefers the use of chemical solvents like monoethanolamine (MEA) for CO_2 absorption, making it very compatible with present infrastructure. Some of the advantages are compatibility with present facilities and easy integration with the existing setup (Fig. 2) [13,15]. It is disadvantageous as it is energy-intensive because of the need to regenerate solvents, resulting in high operating costs [15].

Pre-Combustion Capture

Pre-combustion capture converts fossil fuels into synthesis gas (syngas), followed by a reaction that separates CO_2 and hydrogen. This technology is efficient for integrated gasification combined cycle (IGCC) plants, enabling the direct use of hydrogen as a low-carbon fuel [13,16]. Advantages include high efficiency in CO_2 separation and suitability for hydrogen production. Disadvantages include high initial investment and complex infrastructure, limiting its deployment primarily to new plants [16].

Oxy-fuel Combustion

Oxy-fuel combustion involves burning fossil fuels in pure oxygen instead of air, producing a highly concentrated stream of CO_2 after condensing water vapor. Advantages include simplified CO_2 capture and high purity of captured gas [13,17]. However, this method requires energy-intensive oxygen production, usually by cryogenic air separation, which significantly increases operating costs. Additionally, the technology poses challenges such as material corrosion and operational complexity [17].
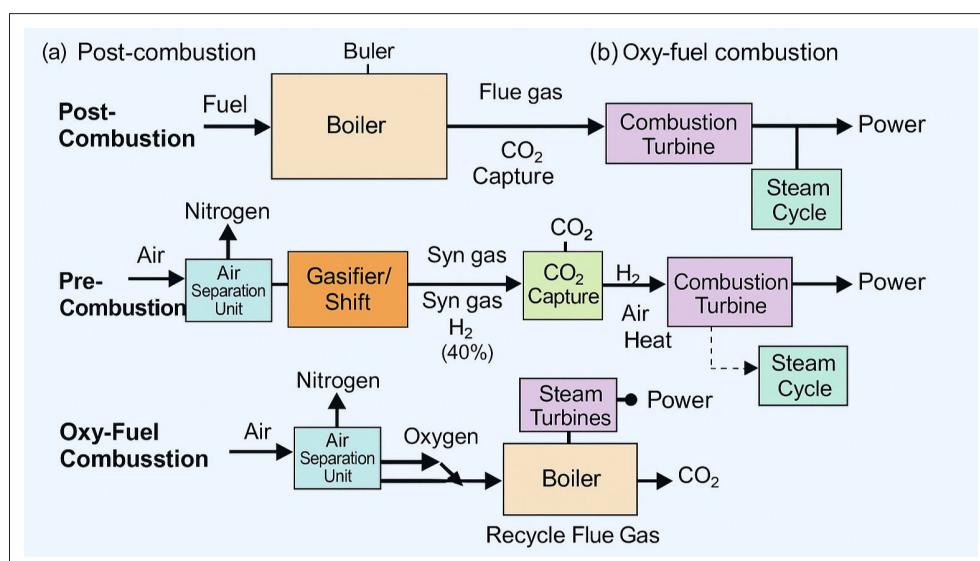

Figure 2. Simplified process diagrams of major CO_2 capture methods: **(a)** Post-combustion, **(b)** Pre-combustion, **(c)** Oxy-fuel combustion. (Redrawn and adapted by the authors based on source [63]).

Alternative Technologies

Emerging CCUS technologies include membrane-based separation, chemical looping combustion (CLC), cryogenic separation, ionic liquid absorption, electrochemical capture, and solid sorbent adsorption (e.g., metal-organic frameworks (MOFs), zeolites). These methods typically offer lower energy requirements and smaller environmental footprints compared to conventional methods, although they often require further development to become economically feasible at scale [18,19].

CCUS Implementation in Türkiye

Türkiye has shown increasing interest in CCUS technologies, particularly after ratifying the Paris Agreement and setting a net-zero emissions target for 2053 [20]. Although commercial-scale deployment is currently limited, TÜBİTAK-supported national projects increasingly focus on CO_2 conversion into value-added products such as biofuels and minerals [20,21]. The EU's Carbon Border Adjustment Mechanism (CBAM) further encourages Türkiye to develop CCUS infrastructure in alignment with both climate and trade goals [14,21].

However, the discussion on Türkiye's CCUS potential has so far remained superficial. Specific data regarding regional CO_2 storage capacities, techno-economic feasibility studies, and measurable outputs from TÜBİTAK-funded or other national pilot projects are currently underrepresented in the literature. For instance, regional geological surveys conducted by MTA and TÜBİTAK suggest that formations such as the Tuz Gölü basin and Diyarbakır–Batman region may offer cumulative CO_2 storage potentials exceeding 1.5 Gt [22,23]. Additionally, the TÜBİTAK 1001 Project titled "Integrated Carbon Capture and Bio-methanation in Anaerobic Systems" (Project Code: 120Y156), as well as Borusan's pilot CO_2 mineralization facility in Gemlik, have reported early techno-economic data including capture costs below \$60/ton CO_2 and energy penalties under 15% [24,25]. Including such information provides a more comprehensive perspective on Türkiye's readiness and potential for CCUS deployment and integration into national decarbonization strategies.

Global Implementation of CCUS

Several countries have advanced CCUS deployment. Notable examples include the Boundary Dam project in Canada, Petra Nova in the USA, and Sleipner in Norway—demonstrating real-world feasibility and climate benefits [26,13]. However, challenges persist regarding cost, infrastructure, and verification of long-term storage. For Türkiye, proactive industrial collaboration and supportive policy frameworks will be key to aligning with international climate and economic targets.

FUTURE PLANS IN THE HYDROGEN PRODUCTION SECTOR

Hydrogen production is rapidly evolving as countries pursue low carbon pathways to meet climate goals. Green and blue hydrogen, in particular, are emerging as key tools in global decarbonization efforts. The sector's long term viability depends not only on innovation but also on strong policy support, infrastructure investment, and financial incentives. This section outlines the future direction of hydrogen production, emphasizing global targets, strategic frameworks, and links to carbon reduction technologies like CCUS.

Strategic Roadmaps and Global Alignment

In line with the Paris Agreement and COP commitments, many nations have introduced national hydrogen plans with clear emission reduction goals and production targets. These roadmaps increasingly integrate hydrogen across sectors such as energy, transport, and industry, reflecting a shared vision of its role in a sustainable energy future. The International Energy Agency (IEA) projects that global hydrogen demand could reach 530 million tonnes by 2050 under its Net Zero Emissions (NZE) scenario, with more than 60% produced from renewable sources [27] as illustrated in Figure 3. The European Union (EU), through its Hydrogen Strategy and REPowerEU plan, aims to install 40 GW of electrolyzer capacity within its borders by 2030 and produce 10 million tonnes of renewable hydrogen annually. This will be complemented by an equivalent volume of hydrogen imports from partner countries. National strategies mirror this ambition. Germany plans to reach 10 GW of electrolyzer capacity by 2030, while France and Spain are targeting 6.5 GW and 4 GW, respectively [28]. In Asia, Japan's Green Growth Strategy sets the goal of establishing a full hydrogen supply chain by 2030, supported by substantial public investment. China, the world's largest hydrogen producer, is actively investing in blue and green hydrogen projects, particularly in industrial hubs. Australia and the United States are also leading the transition. Australia aims to develop up to 50 GW of electrolyzer capacity, positioning itself as a global hydrogen exporter [29], while the U.S. government has initiated the Regional Clean Hydrogen Hubs (H₂Hubs) program with an \$8 billion budget under the Bipartisan Infrastructure Law [30].

Capacity Targets and Infrastructure Development

The scalability of hydrogen production relies on a dramatic expansion of electrolyzer manufacturing, renewable electricity generation, water supply, and transport logistics. For instance, the IEA estimates that reaching global decarbonization targets will require the deployment of over 850 GW of electrolyzers by 2050, a more than 100-fold increase from current levels [30]. Countries are accordingly investing in grid upgrades, port facilities, hydrogen pipelines, and hydrogen-ready industrial zones [31].

In the EU, initiatives such as the European Hydrogen Backbone (EHB) project propose the development of over 40,000 kilometers of dedicated hydrogen transport pipe-
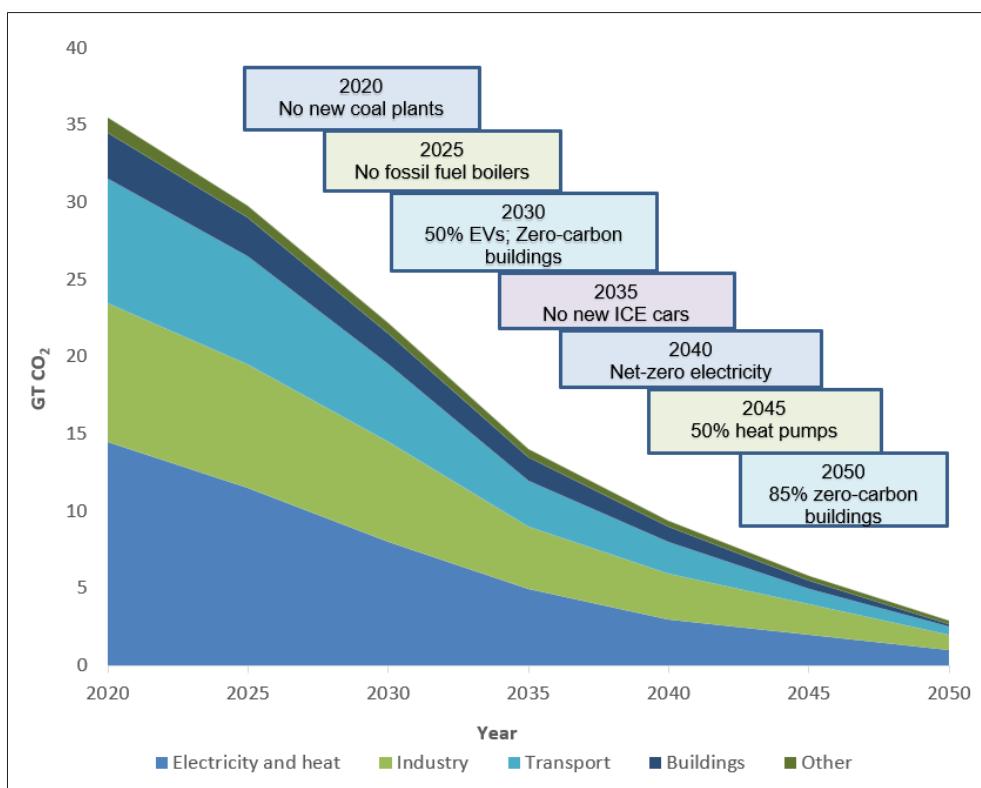
Figure 3. IEA – Net Zero 2050 Roadmap [30].

lines across 28 countries by 2040 [32]. Similarly, Germany is advancing a Hydrogen Core Network that will connect production sites to industrial demand centers. In theUSA, the H₂Hubs are designed not only to establish regional hydrogen markets but also to enable cross-sector integration between industry, mobility, and power generation [30].

Policy and Financial Mechanisms

The realization of hydrogen's potential depends heavily on economic viability and policy support. A variety of mechanisms have been introduced to stimulate investment and de-risk early-stage projects. In the EU, the Emissions Trading System (EU ETS), launched in 2005 and revised in 2023, has raised the cost of carbon to over €85 per tonne, improving the competitiveness of low-carbon hydrogen [33]. Innovation Funds, State Aid Guidelines, and Carbon Contracts for Difference (CCfDs), introduced gradually since 2020, further incentivize green and blue hydrogen production by guaranteeing revenue streams or offsetting operational costs. In the U.S., the 45V production tax credit, introduced under the Inflation Reduction Act (IRA) in 2022, provides up to $3/kg of clean hydrogen produced depending on life-cycle emissions, effectively making green hydrogen cost-competitive with fossil-derived hydrogen [30]. In addition, the 45Q tax credit, first enacted in 2008 and expanded in 2022, provides $85 per tonne of CO_2 captured and stored, directly supporting blue hydrogen projects integrated with CCUS [32].

Asia is also rapidly mobilizing capital. Japan has pledged $13.5 billion in subsidies for hydrogen infrastructure since 2021, while South Korea and China are combining industrial policy with public-private partnerships to scale hydrogen supply chains. Financial institutions are also stepping in; multilateral banks and green investment funds are increasingly supporting hydrogen projects in emerging economies.

Integration with CCUS and Transition Pathways

Although green hydrogen remains the ultimate objective, blue hydrogen produced through SMR combined with CCUS is widely viewed as a practical transition solution. As noted by the Hydrogen Council (2023), blue hydrogen can cut CO_2 emissions by up to 90% compared to conventional grey hydrogen, making it particularly relevant for gas-rich regions [34].

Countries such as Canada, Norway, and the UK have incorporated blue hydrogen into their national strategies, taking advantage of existing gas networks and geological CO_2 storage options. Flagship CCUS projects like Norway's Northern Lights and the UK's Net Zero Teesside are setting examples by integrating hydrogen production with advanced carbon capture systems. Additionally, alternatives like turquoise hydrogen from methane pyrolysis and hydrogen from nuclear-powered electrolysis are gaining attention as region-specific, low-carbon solutions that may bridge the gap toward full decarbonization.

POTENTIAL OF CCUS TECHNOLOGIES IN THE HYDROGEN PRODUCTION SECTOR

Technological and Operational Improvements

Currently, hydrogen is predominantly produced from fossil fuels, namely brown and grey hydrogen. According to the International Renewable Energy Agency (IRENA-2018), approximately 48% of global hydrogen production is derived from natural gas, 30% from oil, and 18% from coal. Only about 4% is generated through electrolysis using electricity from the grid or renewable energy sources, which is referred to as green hydrogen. Hydrogen is currently utilized across various industrial sectors, including chemical production (e.g., methanol, ammonia), refining processes (such as hydrogenation and hydrocracking), metal processing, aerospace, food, and glass industries [35]. In addition to methanol synthesis, hydrogen plays a pivotal role across a range of industrial processes where its high reactivity and energy density are leveraged. Ammonia production, primarily via the Haber–Bosch process, remains one of the most hydrogen-intensive applications globally. This process involves the reaction of nitrogen, extracted from ambient air, with hydrogen under elevated pressures and temperatures in the presence of an iron-based catalyst, and it is fundamental to global fertilizer manufacturing [36]. In the petroleum refining sector, hydrogen is extensively employed in hydrocracking and hydrotreating units to upgrade heavy hydrocarbon fractions, eliminate impurities such as sulfur, nitrogen, and metals, and generate cleaner transportation fuels. Moreover, hydrogenation reactions are widely utilized in the chemical industry to saturate unsaturated organic compounds, thereby enhancing the chemical stability, performance, and shelf life of end products [37]. These hydrogen-driven applications are underpinned by mature and well-established technologies characterized by high Technology Readiness Levels (TRLs). As the global energy system transitions toward low-carbon solutions, these conventional hydrogen-based processes are increasingly being re-evaluated for integration with carbon capture technologies and green hydrogen alternatives to mitigate their environmental impact and contribute to industrial decarbonization [38,39].

Among its various uses, methanol is a "bridge" molecule that enables both the chemical fixation of CO_2 and the practical transportation and storage of H_2. This dual function makes it a strategic intermediate for both carbon management and renewable energy storage/distribution. Methanol (MeOH) is recognized as a key feedstock in the petroleum, chemical, and energy industries. It serves as a fuel in fuel cells, gasoline blending, combustion engines, and marine applications, while also acting as a precursor in the production of acetic acid, formaldehyde, olefins, and synthetic fibers. Owing to its versatile applications, global demand for methanol increased by approximately 4% between 2018 and 2023 [40]. Additionally, due to growing concerns about climate change and increasing interest in hydrogen as a clean energy carrier, methanol has emerged as a viable medium for hydrogen storage and transport. It can be synthesized via a single-step catalytic reaction using CO_2 and H_2 as reactants, allowing for the chemical fixation of CO_2. When derived from captured CO_2 emissions, the resulting product is referred to as blue methanol. Global methanol demand is projected to grow from 100 million tonnes in 2020 to 500 million tonnes by 2050 [35, 40]. Methanol can be classified as either high or low carbon intensity, depending on the feedstock and associated emissions. Methanol produced from fossil fuels such as coal and natural gas, without carbon capture or renewable inputs (i.e., brown and grey methanol), is typically categorized as high-carbon. In contrast, methanol derived from renewable energy, fossil sources with carbon capture, or a combination of both (green and blue methanol), is regarded as a low-carbon alternative.

Conventional methanol production is primarily based on SMR, where synthesis gas (H_2, CO, and CO_2) is generated from natural gas. SMR is the most common and cost-effective method for hydrogen production, used by approximately 50% of global hydrogen production facilities. The resulting synthesis gas can be directly utilized in methanol synthesis, potentially meeting up to 90% of global methanol demand. The technology has reached a high maturity level, reflected in its Technology Readiness Level (TRL) of 9 [41]. In the SMR process, methane (CH_4) reacts with steam at high temperatures to produce H_2 and CO. This is followed by the Water-Gas Shift (WGS) reaction, where part of the CO is converted into CO_2 while additional hydrogen is produced (Figure 4). The resulting gas mixture, rich in H_2 and CO_2, is purified using physical or chemical separation techniques and then used for methanol synthesis in appropriate ratios. The proposed process enables the simultaneous production of both H_2 and CO_2 from natural gas, which are directly utilized for methanol synthesis. This way, carbon from fossil sources is chemically bound in the product rather than being released into the atmosphere, exemplifying an effective application of CCUS technology.

Conventional SMR operates at 800-900 °C and 3-25 bar, requiring partial combustion of natural gas to provide the heat. This reduces energy efficiency and generates additional CO_2 emissions. Electrically heated SMR (e-SMR), on the other hand, reforms hydrocarbons directly with electrical energy by heating the catalytic surfaces by resistance or induction. Using electrical heat instead of combustion eliminates CO_2 emissions from combustion and significantly reduces the carbon intensity of the system [42]. The syngas from the SMR unit is typically directed to gas separation units such as membrane systems, Pressure Swing Adsorption (PSA) or amine absorption, where H_2 and CO_2 are separated into separate phases.
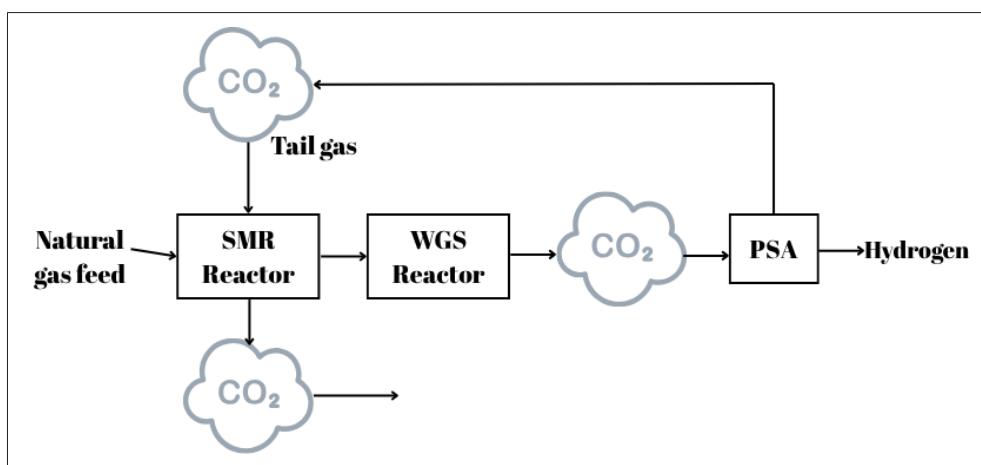
Figure 4. SMR based blue hydrogen and CO_2 production [64].

The new generation of zeolite-based membrane technologies in particular offer high H_2 purity and enable the installation of compact integrated systems, significantly improving operational efficiency. Obtaining the separated CO_2 in a separate phase makes it possible to use this gas directly in chemical bonding or capture processes [43, 44]. The $CO_2 + H_2$ route for methanol synthesis is both kinetically and thermodynamically more challenging compared to the conventional method involving CO; therefore, special catalysts are required. Since the classical Cu/ZnO/Al$_2$O$_3$ system can show instability at high pressure and temperature, ZnZrO$_x$, In$_2$O$_3$-ZrO$_2$ or Ga-doped alternatives have been developed. For example, In$_2$O$_3$-based catalysts exhibit up to 80% CO_2 conversion and over 90% methanol selectivity at 240-270 °C and 30-50 bar conditions. Catalyst choice plays a key role in operational improvements as it directly affects the energy requirements of the process [45]. Since methanol synthesis is exothermic, it is critical to control the heat generated; otherwise catalyst sintering, loss of selectivity or carbon deposition can occur. Micro-channel reactors offer both safe and low energy consumption methanol production using blue hydrogen, with compact designs that provide fast and homogeneous heat transfer [46]. Heat and energy integration is critical in integrated SMR-methanol plants; up to 800 °C synthesis gas heat from the SMR is reused in stages such as the reboiler of the methanol synthesis unit and preheating of feed steam, increasing energy efficiency. In addition, the energy requirements of auxiliary systems such as CO_2 compressors, H_2 transport lines and product condensation units are minimized thanks to the integrated design. Process simulations in the literature show that total process efficiency can be increased to over 70% with such heat recovery strategies [47].

Feasibility and Scalability

The success of proposed technologies to achieve carbon emission reduction targets should not only be limited to their technical feasibility, but should also meet the conditions of

economic sustainability and compliance with market conditions. Although CO_2-methanol synthesis integrated with SMR-based hydrogen production seems technically feasible in the short term, its economic feasibility varies significantly depending on project parameters, regional energy costs and carbon regulations. In this context, the investment costs, operating costs, production efficiency and economic return models of the system should be examined in detail.

As presented in Table 1., SMR plants at TRL 9 can produce hydrogen at capacities ranging from 200-500 tons per day, while ATR and Partial Oxidation (POx) plants can produce hydrogen at capacities ranging from 500-1000 tons per day, providing flexible solutions for both medium and large industrial needs.

SMR processes can be scaled up above a base efficiency of 83% with existing waste heat recovery strategies, while costs ranging from USD 0.9-1.8 per kilogram are supported by the widespread availability and low price of natural gas. Moreover, the availability of global natural gas pipeline and storage infrastructure reduces the need for large-scale infrastructure investment in the commissioning of new plants, lowering capital expenditures (CAPEX) and shortening the payback period. With these characteristics, natural gas reforming technologies stand out as the "what works" option that offers the highest maturity, efficiency, and cost-effectiveness. In the coming period, blue hydrogen production with waste heat integration and carbon capture applications will also become significantly widespread.

RESULTS AND DISCUSSION

Technical Performance Comparison

The technical evaluation of the three selected CCUS technologies—Post-combustion MEA absorption, polymer membrane separation, and oxy-fuel combustion—is summarized in Table 2. MEA absorption achieved the highest capture rate (85–95%) [49] but at a high energy penalty (3.6–3.8

Table 1. Comparison of hydrogen production technologies [41,48].

Technology	Raw material	TRL	Efficiency (%)	Scalability	Levelized Cost of Hydrogen (LCOH)
SMR	Natural gas	9	~83	200–500 ton/day	0.9–1.8 $/kg
ATR	Natural gas	9	~90	500–1000 ton/day	Not determined
POx	Natural gas and waste oil	9	70–80	500–1000 ton/day	Not determined
Gasification	Coal	9	Not determined	500–800 ton/day	1.6–2.2 $/kg
Pyrolysis	Oil and coal	Not determined	Not determined	50 ton/day	2.2–3.4 $/kg
Alkali electrolysis (AE)	Water + Electricity	9	63–71 (cell) 51–60 (system)	<70 ton/day	2.6–6.9 $/kg
Proton conducting membrane electrolysis (PEM)	Water + Electricity	9	60–68 (cell) 46–60 (system)	<300 ton/day	3.5–7.5 $/kg
Solid oxide electrolysis cell (SOEC)	Water + Electricity	6–7	100 (cell) 76–81 (system)	Not determined	5.0–8.5 $/kg

Table 2. CAPEX and O&M cost comparisons.

Process	CAPEX (€/tCO$_2$)	O&M (€/tCO$_2$)	Usage Period (Year)	References
MEA absorption	90–156	41–44	20-30	[49,56]
Polymer membrane	18-44	Not determined	5	[54,56]
Oxy-fuel combustion	30 - 50	15.47	30	[54,55]

GJ/t CO_2) [43] and is fully commercial (TRL 9) [50]. Polymer membranes offered moderate to high capture efficiency (60–95 %) [49] with a lower energy demand (0.7–1.5 GJ/t CO_2) [49] but remain at TRL 7–8 [51], indicating ongoing scale-up challenges. Oxy-fuel combustion provided ~90% capture with an energy load of 200–300 kWh/t O_2 (≈0.72–1.08 GJ/t CO_2 equivalent) [49] at TRL 7 [52]. Although MEA delivers the best capture efficacy, its high energy consumption may limit deployment in energy-intensive sectors. Conversely, polymer membranes and oxy-fuel offer lower energy footprints but require further development or integration to reach full commercialization [53–55].

Economic Assessment

Table 2 presents CAPEX and Operation and Maintenance (O&M) cost comparisons. MEA absorption incurs the highest total cost (90–156 €/t CO_2 CAPEX; 41–44 €/t CO_2 O&M) [49] but benefits from long operational lifetimes (20–30 years) [49]. Polymer membranes exhibit the lowest CAPEX (18–44 €/t CO_2) [56] and minimal O&M—but suffer from short design lives (≈5 years), potentially increasing replacement frequency and total lifecycle costs [54]. Oxy-fuel combustion sits between the two (30–50 €/t CO_2 CAPEX; 15.5 €/t CO_2 O&M; 30 years lifetime) [54,55]. When normalized over a 20-year period, oxy-fuel demonstrates the most balanced cost

Most Feasible Technology and Sectoral Priorities

Considering both technical and economic metrics, oxy-fuel combustion emerges as the most balanced CCUS option for large-scale industrial emitters. Its moderate capture efficiency (≈90%) [49] and mid-range energy and cost figures make it suitable for cement, steel, and power sectors where high-purity O_2 streams are already used. In contrast, polymer membranes are promising for modular, distributed applications (e.g., small NG-fired turbines) where low energy consumption and compact footprint are critical—even if frequent replacements are required [49]. MEA absorption, while technically proven, is best reserved for schemes with access to low-cost steam or waste heat to offset its high regeneration energy [49]. Among carbon capture technologies, MEA (monoethanolamine) absorption stands out as a mature and well-established method, offering very high CO_2 capture rates and a long operational lifetime. However, its main drawback lies in its high energy consumption and elevated operation and maintenance (O&M) costs [49,50]. Another promising approach is the use of polymer membrane systems, which offer advantages such as low energy demand, low capital expenditure (CAPEX), and compact design. Nevertheless, their short membrane lifespan, scalability challenges, and the fact that they are still at a pre-commercial stage (Technology Readiness Level 7–8) limit their widespread application [49,51-53]. Oxy-fuel combustion technology presents a balanced trade-off be-

tween cost and performance. It can be integrated with existing Air Separation Units (ASU) and provides long-term operational stability. On the downside, it requires large volumes of pure oxygen and considerable energy input for ASU operation, which pose significant challenges for practical deployment [54,52,55].

Discussion and Future Perspective

The choice of CCUS technology must align with sectoral priorities. Energy-intensive industries (cement, steel) favor oxy-fuel for its compatibility with high-purity O_2 combustion and stable operation over decades [49,51]. Conversely, distributed power generation and smaller emitters can leverage polymer membranes' low energy footprint and modularity, accepting shorter equipment life [50,51]. MEA absorption remains a benchmark for large post-combustion flue-gas streams where waste heat integration can mitigate its energy costs [49]. Ultimately, a hybrid deployment—combining MEA for base-load capture, membranes for peaking units, and oxy-fuel for new builds—may optimize overall system performance and economic return across diverse industrial applications.

Integrated CCUS technologies are emerging as a key component of the low-carbon energy transition, playing a critical role particularly in the decarbonization of energy-intensive hydrogen-consuming industries. This is mainly because approximately 95% of today's hydrogen is still produced through fossil fuel-based processes [57]. This situation highlights the increasing importance of CCUS technologies in the pursuit of emission reduction targets. In this context, the Shell Quest project in Alberta, Canada demonstrates the technical and economic feasibility of CCUS integration by capturing and injecting underground approximately 1 million tonnes of CO_2 annually through pre-combustion capture in hydrogen production via SMR [58]. Similarly, at the Port Arthur facility in Texas, operated by Air Products, CO_2 released during hydrogen production in refineries is captured and used in Enhanced Oil Recovery (EOR) processes, delivering both climate and economic benefits. The facility has an annual capture capacity of over 1 million tonnes [59].

One of the pioneering initiatives in Europe, the HyNet project in the United Kingdom, aims to capture up to 95% of the CO_2 from blue hydrogen production using natural gas and transport it to offshore storage sites in Liverpool Bay. The project plans to reach an annual capture capacity of 10 million tonnes of CO_2 by 2030 [60]. These examples demonstrate that CCUS technologies can be successfully integrated into hydrogen production processes, enabling the widespread adoption of blue hydrogen. However, high capital costs, infrastructure requirements, and regulatory uncertainties remain significant barriers at this development stage. Despite these challenges, government support, carbon pricing mechanisms, and net-zero commitments are fostering the spread of such investments.

Although there are some barriers at present, the future outlook for CCUS integration technologies holds significant value when considering global energy transition goals. CCUS plays a vital role in reducing CO_2 emissions, especially in grey and blue hydrogen production processes, positioning itself as a bridging technology in the decarbonization of the hydrogen economy [61]. According to the IEA, around 60% of hydrogen must come from low-carbon sources (blue or green) by 2050 to achieve a carbon-neutral energy system, a goal that will largely depend on the widespread deployment of CCUS technologies [27]. Additionally, according to the IEA's 2024 Global Hydrogen Review, approximately 20% of the $3.5 billion USD investment in hydrogen supply projects in 2023 was allocated to CCUS-integrated projects, most of which are concentrated in North America. With increasing CCUS investments, it is projected that up to 60 million tonnes of CO_2 could be captured annually from hydrogen production by 2030 [27]. Nevertheless, cost, infrastructure limitations, and regulatory uncertainties still pose significant obstacles to the widespread adoption of these technologies [62]. On the other hand, the inclusion of CCUS as a core element in strategic hydrogen policies by countries such as China, as well as incentivizing policy instruments like carbon border adjustments, are supporting the future development of these technologies.

CONCLUSION

This study highlights that integrating CCUS technologies into hydrogen production processes can serve as a crucial step in the broader transformation of energy systems. Particularly, the deployment of CCUS within SMR and ATR-based hydrogen production pathways significantly lowers the carbon intensity of hydrogen, providing a realistic and scalable option during the energy transition period. Blue hydrogen, as a result of this integration, presents emission reductions that in some cases reach close to 90% compared to traditional grey hydrogen production.

Different capture methods yield varied technical outcomes. While solvent-based systems like MEA absorption deliver high capture rates, they also introduce notable energy costs. On the other hand, membrane-based systems and oxy-fuel combustion offer operational advantages with lower energy demand, making them suitable for targeted industrial use where energy efficiency is a priority. These technological differences suggest that a mix of capture approaches, tailored to specific sectors, could maximize effectiveness. Another key finding is that using captured CO_2 for methanol synthesis creates additional value, both environmentally and economically. This circular approach supports the green transition by converting emissions into useful chemicals and fuels, reducing reliance on fossil-derived inputs. Countries like Türkiye, which already have es-

tablished natural gas infrastructure, stand to benefit from this interim strategy. It enables immediate emission cuts while building the technical and institutional foundation for a broader shift to green hydrogen in the long term.

Taken together, the results underscore that CCUS-enabled hydrogen systems can act as a bridge—both technologically and strategically—between today's carbon-intensive landscape and tomorrow's net-zero ambitions. The dual alignment with energy transition pathways and green transition goals positions blue hydrogen as a critical piece of the decarbonization puzzle.

AUTHORSHIP CONTRIBUTIONS

Authors equally contributed to this work.

DATA AVAILABILITY STATEMENT

The authors confirm that the data that supports the findings of this study are available within the article. Raw data that support the finding of this study are available from the corresponding author, upon reasonable request.

CONFLICT OF INTEREST

The author declared no potential conflicts of interest with respect to the research, authorship, and/or publication of this article.

ETHICS

There are no ethical issues with the publication of this manuscript.

STATEMENT ON THE USE OF ARTIFICIAL INTELLIGENCE

Artificial intelligence was not used in the preparation of the article.

REFERENCES

[1]   International Energy Agency, The Future of Hydrogen, IEA. Available at: https://www.iea.org/reports/the-future-of-hydrogen Accessed on May 13, 2025.

[2]   International Renewable Energy Agency, Green Hydrogen: A Key Enabler of the Energy Transition, IRENA. Available at: https://www.irena.org/publications, Accessed: Accessed on May 13, 2025.

[3]   Bloomberg New Energy Finance. Global Hydrogen Market Overview, 2023.

[4]   Switzer Manufacturing. Hydrogen Production: Advantages & Disadvantages of Different Methods. Avaialble at: https://www.switzermfg.com/blog/hydrogen-production-advantages-disadvantages-of-different-methods/ Accessed on May 13, 2025.

[5]   World Economic Forum. How Blue Hydrogen is Becoming a Key Strategy for Low-Carbon Energy Transition. Available at: https://www.weforum.org/agenda/2023/07/blue-hydrogen-energy-transition/ Accessed on May 13, 2025.

[6]   Roy R, Antonini G, Hayibo KS, Rahman MM, Khan S, Tian W, et al. Comparative techno-environmental analysis of grey, blue, green/yellow and pale-blue hydrogen production. Int J Hydrogen Energy 2025;116:200–210. [CrossRef]

[7]   Zhang X, Liu Y, Zhang Y, Wang C, Zhao M. Technological evolution of large-scale blue hydrogen production. Nat Commun 2024;15:1234. [CrossRef]

[8]   Natural Resources Canada. Shell Canada Energy Quest Project. Available at: https://natural-resources.canada.ca/funding-partnerships/shell-canada-energy-quest-project Accessed on Jul 27, 2025

[9]   Honeywell. Low-Carbon Hydrogen Production Case Study, Available at: https://ess.honeywell.com/content/dam/ess/en/documents/document-lists/uop/case-study/hon-ess-uop-low-carbon-hydrogen-production-case-study.pdf   Accessed on May 13, 2025.

[10]   Khan MS, Rahman A, Tanveer M. Blue hydrogen production from natural gas reservoirs: A review. J Nat Gas Sci Eng 2023;105:104123.

[11]   Howarth RW, Jacobson MZ. How green is blue hydrogen?, Energy Sci Eng 2021;9:1676–1687. [CrossRef]

[12]   T.C. Enerji ve Tabii Kaynaklar Bakanlığı. Türkiye Hidrojen Stratejisi ve Yol Haritası. Available at: https://enerji.gov.tr/Media/Dizin/SGB/tr/Kurumsal_Politikalar/HSP/ETKB_Hidrojen_Stratejik_Plan2023.pdf Accessed on May 13, 2025.

[13]   International Energy Agency. (2023). CCUS in clean energy transitions. Available at: https://www.iea.org/reports/ccus-in-clean-energy-transitions   Accessed on May 13, 2025.

[14]   Bui M, Adjiman CS, Bardow A, Anthony EJ, Boston A, Brown S, et al. Carbon capture and storage (CCS): The way forward. Energy Environ Sci 2018;11:1062–1176. [CrossRef]

[15]   Wang M, Stephenson P, Ramshaw C. Post-combustion CO_2 capture with chemical absorption: A review. Chem Eng Res Design 2011;89:1609–1624. [CrossRef]

[16]   U.S. Department of Energy. (2022). Carbon capture, utilization, and storage (CCUS). Available at: https://www.energy.gov/fecm/carbon-capture-utilization-and-storage-research Accessed on Jan 06, 2026.

[17]   Koç T, Arslan O. A review on the applicability of carbon capture and storage technologies in Turkiye. J Energy Markets Legislation 2022;15:85–102.

[18]   Chalmers University of Technology. 2022. Chemical

looping research reports. Available at: https://www.chalmers.se Accessed on Jan 06, 2026.

[19] AlgaePARC. 2022. Research projects on bio-based CO_2 capture. https://www.wur.nl/algaeparc Accessed on Jan 06, 2026.

[20] Ministry of Environment and Urbanization of Turkiye. (2021). Paris Agreement and net zero emissions target. Available at: https://www.csb.gov.tr/paris-anlasmasi-ve-net-sifir-emisyon-hedefi Accessed on Jan 06, 2026.

[21] TÜBİTAK Marmara Research Center. R&D activities on carbon capture and utilization technologies. Ankara: The Scientific and Technological Research Council of Turkiye (TÜBİTAK), 2022.

[22] Maden Tetkik ve Arama Genel Müdürlüğü. Türkiye'nin Bölgesel CO_2 Depolama Kapasite Haritası ve Jeolojik Uygunluk Raporu. Ankara: MTA Yayınları; 2022.

[23] Türkiye Bilimsel ve Teknolojik Araştırma Kurumu (TÜBİTAK) Marmara Araştırma Merkezi. Karbon Yakalama, Kullanım ve Depolama (CCUS) Teknolojileri Kapsamında Türkiye'nin Teknik Potansiyeli. Kocaeli: Enerji Enstitüsü Yayını; 2021.

[24] Borusan Ar-Ge. Gemlik CO_2 Mineralizasyon Pilot Tesisi: Teknik ve Ekonomik Değerlendirme Raporu. İstanbul: Borusan Holding Yayınları; 2023

[25] TÜBİTAK. Integrated Carbon Capture and Bio-Methanation in Anaerobic Systems (Proje No: 120Y156). TUBITAK ARBIS Proje Portalı. 2020. Availeble at: https://arbis.tubitak.gov.tr Accessed on Jan 06, 2026.

[26] Global CCS Institute. The global status of CCS 2023. Available at: https://www.globalccsinstitute.com/resources/global-status-report/ Accessed on Jan 06, 2026.

[27] International Energy Agency (IEA). (2021). Net Zero by 2050: A Roadmap for the Global Energy Sector. Available at: https://www.iea.org/reports/net-zero-by-2050 Accessed on Jan 06, 2026.

[28] International Renewable Energy Agency (IRENA). (2023). World Energy Transitions Outlook 2023. Available at: https://www.irena.org/publications Accessed on Jan 06, 2026.

[29] Bloomberg New Energy Finance (BNEF). Hydrogen economy outlook. 2023. Available at: https://about.bnef.com/blog/hydrogen-economy-outlook/ Aceesed on May 14, 2025.

[30] U.S. Department of Energy (DOE). Regional Clean Hydrogen Hubs. 2023. Available at: https://www.energy.gov/oced/regional-clean-hydrogen-hubs Accessed on May 14, 2025.

[31] European Hydrogen Backbone (EHB). (2023). EHB vision. Available at: https://www.ehb.eu/ Accessed on May 14, 2025.

[32] U.S. Department of Energy (DOE). 45Q Carbon Capture Tax Credit. 2022. Available at: https://www.energy.gov/fecm/45q-carbon-capture-tax-credit Accessed on May 14, 2025.

[33] European Environment Agency (EEA). EU Emissions Trading System data viewer. 2023. Available at: https://www.eea.europa.eu Accessed on May 14, 2025.

[34] Hydrogen Council. Hydrogen Insights 2023. Available at: https://hydrogencouncil.com/en/hydrogen-insights-2023 Accessed on May 14, 2025.

[35] IRENA. Hydrogen from renewable power. Technology Outlook for the Energy Transition, International Renewable Energy Agency, Abu Dhabi. 2018. Accessed on April 18, 2025.

[36] Morlanés N, Katikaneni SP, Paglieri SN, Harale A, Solami B, Sarathy SM, et al. A technological roadmap to the ammonia energy economy: Current state and missing technologies. Chem Eng J 2021;408:127310. [CrossRef]

[37] Moradpoor I, Syri S, Santasalo-Aarnio A. Green hydrogen production for oil refining–Finnish case. Renew Sustain Energy Rev 2023;175:113159. [CrossRef]

[38] International Energy Agency (IEA). The Future of Hydrogen. 2019. Available at: https://www.iea.org/reports/the-future-of-hydrogen. Accessed on July 21, 2025.

[39] International Energy Agency IEA. Achieving Net Zero Heavy Industry Sectors. Available at: https://www.iea.org/reports/achieving-net-zero-heavy-industry-sectors-in-g7-members. Accessed on July 21, 2025.

[40] Methanol Institute. Methanol price and supply/demand. 2025. Available at: https://www.methanol.org/methanol-price-supply-demand/ Accessed on April 20, 2025

[41] AlHumaidan FS, Halabi MA, Rana MS, Vinoba M. Blue hydrogen: Current status and future technologies. Energy Convers Manag 2023;283:116840. [CrossRef]

[42] Wismann ST, Engbæk JS, Vendelbo SB, Bendixen FB, Eriksen WL, Aasberg-Petersen K, et al. Electrified methane reforming: A compact approach to greener industrial hydrogen production. Science 2019;364:756–759. [CrossRef]

[43] Naquash A, Qyyum MA, Chaniago YD, Riaz A, Sial NR, Islam M, et al. Membrane-and-Cryogenic-Assisted Hydrogen Separation and Purification Process. Energy Proceed 2021;24:0241. [CrossRef]

[44] Naquash A, Qyyum MA, Chaniago YD, Riaz A, Yehia F, Lim H, et al. Separation and purification of syngas-derived hydrogen: A comparative evaluation of membrane-and cryogenic-assisted approaches. Chemosphere 2023;313:137420. [CrossRef]

[45] Frei MS, Mondelli C, García-Muelas R, Kley KS, Puértolas B, López N, et al. Atomic-scale engineering of indium oxide promotion by palladium for methanol production via CO_2 hydrogenation. Nat Commun 2019;10:3377. [CrossRef]

[46] Delsman ER, Laarhoven BJPF, De Croon MHJM, Kramer GJ, & Schouten JC. Comparison between conventional fixed-bed and microreactor technology for a portable hydrogen production case. Chem Eng Res Design 2005;83:1063−1075. [CrossRef]

[47] Pak KS, Hong YS. Potential environmental impact evaluation of the methanol synthesis process by gas-to-methanol technology. ACS Omega 2025;10:13228−13235. [CrossRef]

[48] KFAS White paper. towards a hydrogen strategy for Kuwait. Kuwait Foundation for the Advancement of Sciences: Kuwait; 2021. p. 92.

[49] Bertone M, Stabile L, Cortellessa G, Arpino F, Buonanno, G. Techno-economic assessment of amine-based carbon capture in waste-to-energy incineration plant retrofit. Sustainability 2024;16:8468. [CrossRef]

[50] Sreńscek-Nazzal, J, Kiełbasa K. Advances in modification of commercial activated carbon for enhancement of CO_2 capture. Appl Surf Sci 2019;494:137−151. [CrossRef]

[51] Pasichnyk M. Membrane Technology for challenging separations: Removal of CO_2, SO_2 and NOx from flue and waste gases. Sep Purif Technol 2023;323:124436. [CrossRef]

[52] Nemitallah MA, Habib MA, Badr HM, Said SA, Jamal A, Ben-Mansour R, et al. Oxy-fuel combustion technology: Current status, applications, and trends. Int J Energy Res 2017;41:1670−1708. [CrossRef]

[53] Seo SB, Kim HW, Kang SY, Go ES, Keel S. Techno-economic comparison between air-fired and oxy-fuel circulating fluidized bed power plants with ultra-supercritical cycle. Energy 2021;233:121217. [CrossRef]

[54] García-Luna S, Ortiz C, Carro A, Chacartegui R, Pérez-Maqueda LA. Oxygen production routes assessment for oxy-fuel combustion. Energy 2022;254:124303. [CrossRef]

[55] Tranier J-P, Dubettier Richard, Darde A, Perrin N. Air separation, flue gas compression and purification units for oxy-coal combustion systems. Energy Proceed 2011;4:966−971. [CrossRef]

[56] Watson JC, Pennisi KJ, Parrish C, Majumdar S. Techno-economic process optimization for a range of membrane performances: What provides real value for point-source carbon capture?" Carbon Capture Sci Technol 2024;11:100182. [CrossRef]

[57] IEA. Global Hydrogen Review 2023. International Energy Agency. 2023. Available at: https://www.iea.org/reports/global-hydrogen-review-2023 Accessed: 12 May 2025.

[58] Shell Quest Carbon Capture and Storage Project: Annual Report. 2022. https://www.shell.ca Accessed on 12 May 2025.

[59] Global CCS Institute. CO_2RE Database: Port Arthur CCS Project Profile. 2023. Available at: https://co2re.co Accessed on May 14, 2025.

[60] HyNet. HyNet North West: Low Carbon Hydrogen and Carbon Capture Project Overview. 2024. Available at: https://hynet.co.uk Accessed on May 14, 2025.

[61] Song C, Zhao Z, Liu Z. Evaluation of regional and temporal dynamics in CCUS-hydrogen development policy pathways: A data-driven framework. Renew Energy 2024;200:1500−1515.

[63] IRENA. Carbon Capture and Storage in Hydrogen Production: Technology Brief. International Renewable Energy Agency. 2022. https://www.irena.org/publications/2022/Mar/CCS-in-hydrogen-production Accessed on May 14, 2025.

[64] Rubin ES, Davison JE, Herzog HJ. The cost of CO_2 capture and storage. Int J Greenhouse Gas Control 2015;40:378−400. [CrossRef]

[65] Li R, Kawanami H. A recent review of primary hydrogen carriers, hydrogen production methods, and applications. Catalysts 2023;13:562. [CrossRef]

Technical Note

Establishing a pioneering laboratory for second-life battery applications: Enhancing energy storage and reducing environmental impact

Murat AKKUŞ[1] , **İbrahim ESKİ[2*]** , **Ali Rıfat BOYNUEĞRİ[1,2]**

[1]Department of Electrical Engineering, Yildiz Technical University, Istanbul, Türkiye
[2]Clean Energy Technologies Institute, Yildiz Technical University, Istanbul, Türkiye

ARTICLE INFO

ABSTRACT

Battery technologies are important in advancing energy storage systems (ESS), particularly focusing on transitioning from end-of-life to second-life applications. This paper explores a variety of battery types including lead acid, lithium-ion, nickel-cadmium, and nickel-metal hydride, detailing their characteristics, applications, and the recycling challenges they present. Special emphasis is given to lithium-ion batteries due to their high energy density and widespread use in electric vehicles and portable devices. The limited lifespan of these batteries highlights significant economic and environmental challenges, emphasizing the necessity for efficient second-life usage and improved recycling strategies. To address these challenges, the establishment of a specialized battery research laboratory is proposed. The laboratory aims to enhance battery lifespan, optimize designs for second-life use, and advance recycling processes. Positioned as an innovation hub, this laboratory is expected to drive advancements in battery technology, fostering sustainable and economically viable energy solutions. The integration of theoretical analyses with practical case studies offers a comprehensive look at the current state and future potential of battery technology in ESS, underscoring its importance in achieving a more sustainable energy future.

Cite this article as: Akkuş M, Eski İ, Boynueğri AR Establishing a pioneering laboratory for second-life battery applications: Enhancing energy storage and reducing environmental impact. Clean Energy Technol J 2025;3(2):62–72.

INTRODUCTION

Due to technological advances and the increasing reliance on intermittent renewable sources like solar and wind, energy storage has become a crucial component of grid systems. Energy storage systems (ESS) are important technologies that enable the storage and conversion of electrical energy in different forms. Although various ESS such as supercapacitors and hydroelectric storage exist, batteries have become the most prevalent, particularly in electric vehicles (EVs), portable devices, and power grids. This widespread adoption is due to their ability to provide an environmentally friendly option for energy storage [1].

To reduce the negative effects caused by long-term use of traditional energy sources, clean energy sources have come to the fore in the fields of energy production and consumption. By encouraging the use of clean energy, elec-

*Corresponding author
*E-mail adress: ibrahim.eski@yildiz.edu.tr

trification has become widespread in every field. However, the inability to store energy on a large scale has been a significant obstacle in this field. To overcome this obstacle, batteries have become critical for industrial and consumer applications, and their technology is constantly evolving. Next-generation batteries offer higher energy density and performance than traditional batteries [2].

In the battery industry, battery types such as Lead Acid (Pb-Acid), Lithium Ion (Li-ion), Nickel-Cadmium (NiCd) and Nickel-Metal Hydride (NiMH) are generally used [3]. In Lead Acid batteries, Pb is used as the cathode, Lead Dioxide (PbO_2) as the anode and sulfuric acid (H_2SO_4) as the electrolyte. $PbSO_4$ is formed in the reaction between lead dioxide and lead during charging. During discharge, this reaction occurs in reverse. This type of battery has low energy density but is suitable for high current applications. Besides, it is safe and low cost [4]. Lithium-ion batteries use lithium as the cathode, graphite (C) as the anode, and solid polymer electrolytes or liquid electrolytes as the electrolyte. During charging, lithium ions pass from the cathode to the anode. During discharge, this reaction occurs in reverse. These types of batteries have a high energy density, long life cycle, and are lightweight, but they have some disadvantages in terms of thermal stability, safety, and cost [5,6]. In Nickel-Cadmium batteries, nickel oxide-hydroxide is used as the cathode, cadmium is used as the anode, and aqueous alkaline solutions are used as the electrolyte. During charging, electrons flow from the nickel oxide-hydroxide cathode to the cadmium anode. During discharge, this reaction occurs in reverse. These types of batteries have high energy density and long cycle life, but they have disadvantages such as memory effect, environmental effects of cadmium and not being suitable for low current discharge [7,8]. Nickel-Metal Hydride batteries use nickel oxide-hydroxide as the cathode, metal hydride as the anode, and potassium hydroxide as the electrolyte. During charging, electrons flow from the nickel oxide-hydroxide cathode to the metal hydride anode. During discharge, this reaction occurs in reverse. While these types of batteries have advantages such as high energy density, high-rate capability, no memory effect and high tolerance against overdischarge, they have disadvantages such as self-discharge, charging efficiency and low life cycle [3,7]. Table 1 shows the compari-

Highlights

- Second-life battery applications extend the usability of end-of-life (EOL) batteries in energy storage systems, reducing waste and supporting sustainability.

- Challenges in battery recycling include high costs and inadequate facilities, emphasizing the need for efficient second-life usage over traditional recycling methods.

- The proposed laboratory aims to optimize battery designs for first and second use, focusing on extending lifespan and enhancing performance.

son of the mentioned batteries in terms of nominal voltage, power density, energy density, charging efficiency, life cycle, self-discharge rate, charging temperature, discharging temperature [3, 9].

Among these commonly used battery types, the most used battery type is lithium-ion batteries. These batteries are preferred in many portable devices and vehicles because they have high energy density, longer cycle life, low mass, and low self-discharge rate [5,6]. Lithium-ion batteries can be classified according to the use of different cathode materials. The use of different cathodes brings different features, advantages and disadvantages, and leads to significant variations in key performance metrics such as cycle life. This is why, as seen in Table 1, Li-ion batteries show a wide distribution in cycle life, ranging from 600 to 3000. According to different cathode types, lithium-ion batteries can be classified as follows: Lithium Nickel Manganese Cobalt Oxide ($LiNiMnCoO_2$ or NMC), Lithium Iron Phosphate (LFP), Lithium Nickel Cobalt Aluminum Oxide ($LiNiCoAlO_2$ or NCA), Lithium Manganese Spinel (LMO), Lithium Titanate (LTO), Lithium Nickel Alloys (Li-Ni).

NMC cathode used in Lithium Nickel Manganese Cobalt Oxide ($LiNiMnCoO_2$) batteries uses a mixture containing the elements nickel, manganese, and cobalt. By adjusting the proportions of the elements in the NMC cathode composition, it is possible to produce materials with varying characteristics. [10]. Lithium Iron Phosphate (LFP) is generally preferred for high safety and low cost, but its energy density is slightly lower than other lithium-ion battery types [11]. Lithium Nickel Cobalt Aluminum Oxide (NCA)

Table 1. Comparison of some battery technologies.

Battery type	Nominal voltage (V)	Power density (W/kg)	Energy density (Wh/kg)	Charging efficiency (%)	Cycle life	Self-discharge rate (%/month)	Charging temperature (°C)	Discharging temperature (°C)
Li-ion	3.2–3.7	250–680	100–270	80–90	600–3000	3–10	0 to 45	-20 to 60
NiCd	1.2	150	50–80	70–90	1000	20	0 to 45	-20 to 65
Lead Acid	2	180	30–50	50–95	200–300	5	-20 to 50	-20 to 50
NiMH	1.2	250–1000	60–120	65	300–600	30	0 to 45	-20 to 65

uses a mixture containing the elements nickel, cobalt, and aluminum. These cathodes are generally preferred for high energy density and long life cycle [12]. Lithium Manganese Spinel (LMO) contains lithium manganate ($LiMn_2O_4$). These batteries are generally preferred for low cost and high safety. However, they are also noted for their capacity fade during cycles, particularly at high temperatures [13]. Lithium Titanium Oxide (LTO) contains lithium titanat ($Li_4Ti_5O_{12}$). These batteries are generally preferred for their high safety, long cycle life and fast charge/discharge features [14]. Lithium Nickel Alloys (Li-Ni) contain alloys of lithium and nickel in various proportions. These batteries are generally preferred for their high energy density and low cost [15]. Table 2 shows the comparison of the lithium-based battery types mentioned above in terms of cathode material, anode material, nominal voltage, cycle life, energy density, cost and safety. In addition, comparisons of the relevant battery types in terms of energy density and specific energy are given in Figure 1 [3,16].

The growing adoption of EVs and the development of higher-capacity batteries are key drivers behind the increasing prevalence of battery usage. However, currently the lifespan of the batteries is not at the desired levels. This situation prevents the full potential of developments in battery technology from being used. The short lifespan of batteries causes increased costs and difficulties in achieving sustainability goals. In addition, batteries that have been retired from use pose a major waste problem because they contain environmental risks due to their chemical structure. Especially with the widespread use of EVs, it is expected that a significant amount of used EV batteries will emerge in the coming years. This situation further increases the importance of waste battery management and second-life battery (SLB) applications.

The increasing cumulative capacity of used EV batteries shows that the importance of second-use batteries is increas-
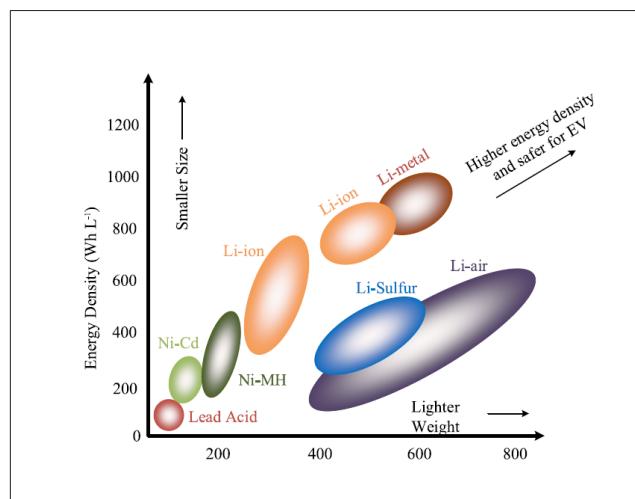

Figure 1. Energy density and specific energy comparison of different batteries [3].

ing and that they have a supporting role in ESS. Figure 2 shows how the supply of second-life lithium-ion batteries is today and where it is expected to reach by 2030 [17].

Although recycling of batteries is very important in terms of providing the raw materials required for battery production, it has remained far from being a solution to the waste battery problem because of the reasons like the lack of advanced recycling techniques for each battery chemistry, lack of global or regional waste battery collection networks, high recycling costs, and the inadequacy of recycling facilities. Instead, reusing batteries after their first use (i.e. second-life usage) makes a great contribution to solving the waste battery problem [18]. In addition, batteries, which still have the potential to provide high energy after their first use, only separate the valuable metals and similar materials they contain through recycling, meaning that their potential is mostly lost.

Table 2. Comparison of the lithium-based battery types.

| Battery type	Anode material	Nominal voltage (V)	Cycle life	Energy density (Wh/L)	Cost	Safety
Lithium Iron Phosphate ($LiFePO_4$)	Graphite	3.2	High	Low	High	Safest Li-ion cell chemistry
Lithium Cobalt Oxide ($LiCoO_2$)	Graphite	3.6	Medium	High	Low	Highest safety concern
Lithium Nickel Manganese Cobalt Oxide ($LiNiMnCoO_2$)	Graphite	3.6	Medium	High	Medium	Good safety
Lithium Manganese Oxide ($LiMn_2O_4$)	Graphite	3.7	Low	Low	Medium	Good safety
Lithium Nickel Cobalt Aluminum Oxide ($LiNiCoAlO_2$)	Graphite	3.6	High	High	Medium	Safety concern required
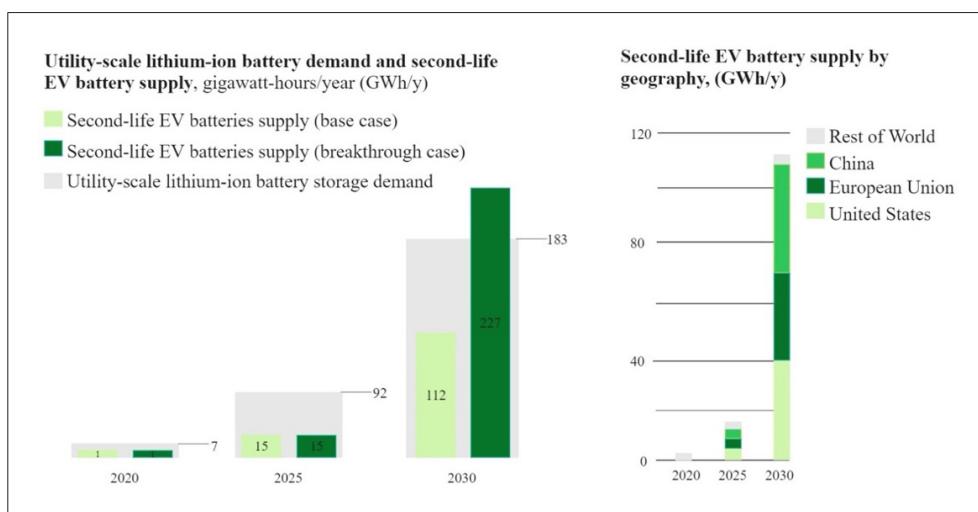
Figure 2. Second-life lithium-ion battery supply: Present and future.

Second-life applications include evaluating used batteries in ESS, power backup systems, renewable energy integration, and other areas. In addition to extending battery life, these applications help utilize resources more effectively and reduce environmental impacts. Additionally, second-life applications are economically advantageous because the value and performance of used batteries can still be maintained. Therefore, considering and encouraging second-life applications during battery design and usage stages is an important strategy to create a sustainable battery ecosystem. This approach should be considered an important step towards a more sustainable future, both environmentally and economically.

In this context, various studies have explored how second-life batteries can be effectively reused in different sectors. These studies examine the technical feasibility, economic viability, and environmental benefits of second-life scenarios in real-world applications. Table 3 provides an overview of literature studies that explore how second-life EV batteries are used in various scenarios [19].

Laboratories investigating the optimal design of batteries in the first and second use stages, aging tests and second use possibilities, and studies conducted in this field, increase awareness about the efficient use of batteries and enable an important step to be taken for an environmentally friendly energy future. In this process, critical parameters such as battery chemistry, size, cover, and cooling system must be optimized by considering the relevant constraints and requirements [42]. Thanks to these optimized parameters, the batteries will exhibit the desired performance and minimize the materials used while providing maximum performance and life. This approach will support sustainability and efficiency goals by making significant contributions to the world ecosystem. Additionally, it will facilitate the integration of renewable energy sources and increase energy efficiency by increasing the ESS' efficiency.

Many companies operate in the field of battery design and optimization. However, services for the optimal design of batteries used in second-life applications are not yet widely available. Batteries with secondary use potential play an important role in ESS and other applications. Therefore, specially designed services are needed to increase the performance, efficiency and durability of end-of-life (EOL) batteries [43]. These services must consider factors such as battery chemistry, capacity management, storage conditions and safety to ensure that batteries use their second life in the most efficient way. Encouraging R&D studies in this field will make significant contributions to an economy that adopts an environmentally sustainable approach.

Infrastracture, Technological Capacity of the Laboratory and Research & Development Activities

Battery technologies are becoming increasingly crucial worldwide, especially in EVs, renewable energy integration, and energy storage. This rapid advancement has created a strong demand for qualified personnel skilled in battery design, production, testing, and second-life applications, as well as R&D. Collaboration between academia and industry plays a vital role in training these experts. Organizing specialized training programs, workshops, and knowledge-sharing platforms will help develop young talent and foster innovation. Strengthening human resources in battery technologies is essential for building a sustainable future.

Battery testing laboratories and a limited number of battery aging laboratories are established in many areas, including the private sector. However, many of these laboratories were established for the purpose of producing battery cells, producing battery stacks from cells, or testing batteries for specific usage needs. The lack of an impartial and non-profit central battery design laboratory is felt. These laboratories are generally designed to suit the specific needs of the organizations. However, there is no laboratory that can record

Table 3. Overview of application scenarios and cases of second-life EVBs.

Category	Application Scenario	Function	Reference
Power generation	Renewable energy power station	Renewable energy integration, smoothing control, reducing curtailed electricity	Wind-Hamidi et al. [20], Alhadri et al. [21], BYD [22], PV-Koch-Ciobotaru et al. [23], Saez-de-Ibarra et al. [24], Leung [25], Fitzpatrick [26]
Grid	Power transmission and distribution network	Alleviate grid congestion, offer ancillary support to the network, and delay the expansion of power transmission and distribution capacity	Neubauer et al. [27], Lacey et al. [28], Eyer and Corey [29]
End-user	Communication base station,	Backup power stage	Li [30], Yan [31]
	EV charging stations,	EV charging	Jiao et al. [32], Han et al. [33], Kamath et al. [34]
	Mobile energy storage device,	Community EV charging Power supply for camping trailers	Potevio New Energy [35]
	Low-speed electric vehicle,	EV energy storage	Nissan Energy [36]
	Street lamp	Energy storage for lamp	Zhang et al. [37], Zhao [38]
	Uninterrupted Power Systems (UPS)	Emergency power	Zhu et al. [39]
	Residential energy storage	Emergency power, reduce electricity costs	Canals Casals et al. [40], Neubauer et al. [41]

battery data for all types of battery cells and environmental conditions, match and make sense of these data using artificial intelligence, test next-generation battery technologies at the cell level and report their performance according to environmental conditions. Moreover, a laboratory that details the optimal application selection, sizing and pricing for the reuse of batteries by considering second-life applications will have a unique position internationally.

As a result, increasing battery usage and their short lifespan leads to serious economic problem due to the use of rare-earth elements. To solve this problem, it is important to use resources in the most efficient way. The second use offers the potential to be used in other applications for up to 8-10 years after the batteries have reached their EOL [44]. However, the second use issue is not yet widespread and faces various obstacles including concerns about planning, security, financial management, and market acceptance. These factors are important challenges that need to be overcome for second use applications to become widespread and potential opportunities to be utilized [45].

The battery laboratory to be established will address the interests of a wide range of sectors that use batteries including important areas such as white goods, EVs, micromobility, telecommunications, defense industry, space industry, and electricity distribution, production, and transmission. These sectors will both play a role as customers for battery design and development and become battery providers for second-life use. In this way, batteries that have reached the end of their first life in one sector can be used as cheap energy storage units in other sectors. This will create an eco-

system and enable the recycling and reuse of batteries with reduced capacity.

This approach aims to use resources more efficiently and ensure environmental sustainability. Moreover, in some cases, the needs of battery firms are based solely on data. Rather than each company setting up separate laboratories, a centralized facility offering data and testing services can more effectively meet sector requirements. Furthermore, inefficiencies and flawed designs stemming from the lack of competent personnel increase costs and reduce the battery performance.

Especially in products that go directly to the end-user, high battery costs cause decision changes and raise questions in terms of reliability. Batteries that have completed their first life in applications that require high C ratio, power and energy density, such as EV and defense and space industries, can be used for another 8-10 years in applications that do not have volume and weight problems, such as UPS and grid level storage systems. However, this opportunity cannot be utilized due to lack of testing, analysis and experts.

The laboratory to be established will enable next-generation battery materials to be tested in real application conditions in cell form. This step will accelerate the transformation of materials into commercial products and enable processes such as valuation and sale of patents. Moreover, academic and R&D studies on second-life applications are limited and there is not enough data for realistic aging processes of batteries. There is a lack of data, especially regarding the performance of aged batteries in applications and the parameters required for design. With the establishment

of the laboratory, aging data will be collected and analyzed in this regard. These data will constitute an important resource for second-life applications of batteries and will support the industry's efforts in this field.

In universities and R&D centers, a lack of scientists and employment in the relevant field is observed. These institutions have difficulties in recruiting qualified personnel. It is aimed for universities and R&D centers to meet this need with activities such as establishing laboratories, in-house internships, trainings and personnel exchange. In this way, competent personnel will be provided to the sector and research and development studies will be carried out more efficiently. In addition, training and information sharing through laboratories will contribute to the strengthening of universities and R&D centers in their areas of expertise.

In Figure 3, the important stages in the battery laboratory to be established is given. The process begins at the cell and stack levels, where monitoring of internal resistance, thermal and mechanical design, and appropriate storage conditions are critical to ensure baseline performance. During storage and operation, the battery is exposed to temperature variations, state-of-charge changes, and aging, which affect overall capacity and reliability. Electrical and thermal protections must be implemented to ensure safe operation over a prolonged period, ideally up to ten years.

As batteries retire from their first life, proper evaluation during vehicle parking duration allows early identification of degradation patterns. In the second-life stage, economically viable reuse applications are explored in consumer electronics, small-scale e-mobility, or ESS. Finally, environmentally responsible recycling is essential to recover valuable materials like nickel, manganese, and lithium while minimizing waste. Each phase in this cycle forms a critical part of the second-life battery workflow.

Subunits of the Laboratory

The aim of this project includes the establishment of various subunits to promote developments in battery technologies and support specialization in this field. In line with this objective, a total of nine interconnected subunits have been designed to cover the entire lifecycle of batteries—from performance evaluation and second-life optimization to economic assessment, user awareness, and training. These subunits collectively form a comprehensive and multidisciplinary research and development infrastructure that can support both industrial and academic needs in the battery sector. The overall system architecture is given in Figure 4.

Each subunit has been structured to fulfill a specific role within this ecosystem. These include the Cell Aging Subunit, Stack Analysis and Aging Subunit, Battery Design and Optimization BMS Design Subunit, Data and Visualization Center, Next-Generation Battery Test Subunit, Economic Battery Management System Subunit, Training Center, and Awareness Center. Additionally, the infrastructure is supported by a mobile application interface designed to make battery monitoring accessible to all user profiles.

The Cell Aging Subunit aims to conduct research to increase batteries' performance and lifespan by examining the aging processes of battery cells. The obtained here will be held in the database and used in the Battery Design Center of the laboratory, and designs for the second use will be based on these data. This subunit will also play an important role in testing the durability of battery materials and structures for long-term use and monitoring their performance.

The Stack Analysis and Aging Subunit of the laboratory is dedicated to evaluating the performance and aging behavior of battery stacks composed of multiple cells. By subjecting these stacks to various charge/discharge cycles, thermal conditions,


Figure 3. Important stages in the battery laboratory to be established.
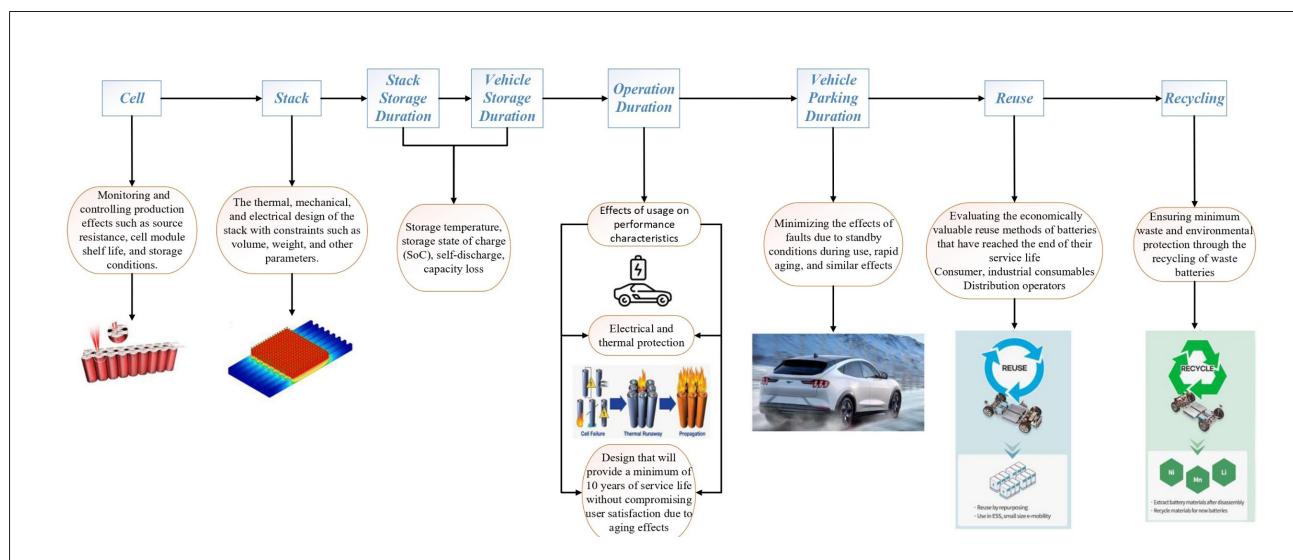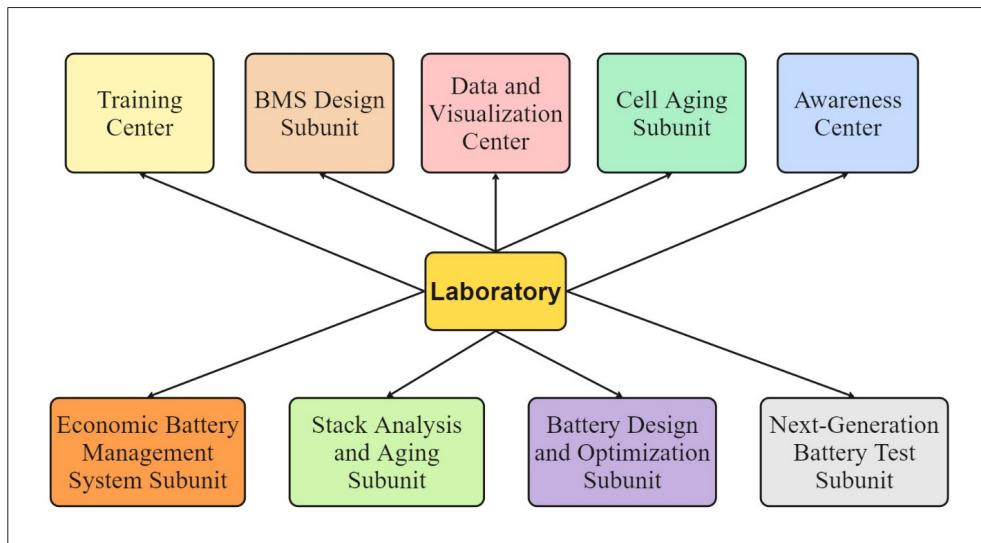
Figure 4. The subunits of the laboratory.

and usage profiles, this unit aims to identify degradation patterns and performance losses over time. The test results will help determine the suitability of these stacks for continued use or second-life applications. Moreover, the findings from this subunit will support the development of standardized testing protocols and contribute to the design of safer and more durable battery systems suited for daily-use scenarios.

The Battery Design and Optimization Subunit aims to increase the energy density, efficiency, and reliability of battery systems by employing advanced design and optimization techniques. This subunit will not only support internal R&D activities but also offer external battery design services for industrial and institutional partners. Initially, its primary focus will be on the design and optimization of newly developed battery systems, where various parameters such as cell configuration, thermal control, and electrical layout will be fine-tuned to meet application-specific requirements. In addition to new battery designs, the subunit will also play a key role in the reuse of aged batteries by utilizing performance and aging data collected from other laboratory units. By incorporating this data into the design process, the subunit will develop second-life battery systems that are both cost-effective and operationally safe. This dual-function approach—addressing both first-life and second-life battery design needs—positions the subunit as a critical component in achieving a circular battery economy and promoting sustainable energy storage practices.

Figure 5 illustrates the conceptual structure of the smart Battery Management System (BMS) developed within the BMS Design Subunit. This unit is dedicated to enhancing battery safety, performance, and lifespan by focusing on the design and optimization of advanced BMS architectures. A key approach involves leveraging large-scale data acquired from battery testing processes, which is then analyzed using artificial intelligence and deep learning algorithms. Through

this data-driven strategy, the system can predict battery health status and remaining useful life with improved accuracy. In addition to its AI-driven capabilities, the smart BMS incorporates a modular hardware and software design, enabling flexible integration and rapid prototyping. As seen in the figure, the platform utilizes next-generation, high-efficiency hardware components that contribute to power savings and increased reliability. Furthermore, an integrated approach underpins the entire system, ensuring cohesive operation among sensing, control, and communication layers.

The Data and Visualization Center is a subunit that aims to facilitate the monitoring and control of battery systems
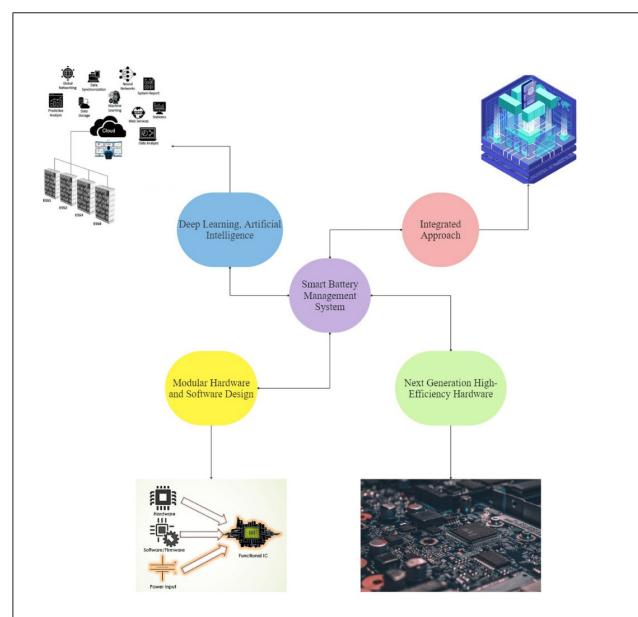

Figure 5. The block diagram of smart Battery Management System (BMS).

by collecting and analyzing data on battery performance and presenting them in a way that is understandable to users. In addition, the data in this center will be processed with artificial intelligence and form the infrastructure of the software to be used in BMSs.

The Next-Generation Battery Test Subunit is designed to establish a comprehensive and advanced testing infrastructure for evaluating the performance, durability, and safety of innovative battery technologies. Within this unit, developed battery materials are first assembled into test cells, which are then subjected to controlled testing conditions using a climate control chamber to simulate various environmental parameters such as temperature and humidity. The electronic load/source unit applies dynamic charge/discharge profiles to the battery cells, while a main computer provides real-time signal control and data acquisition. All measurement results—such as voltage, current, temperature, and capacity—are recorded and analyzed through integrated software tools. After testing, the center delivers detailed technical reports and performance evaluations, enabling standardization and benchmarking of next-generation battery cells under aging and operational stress conditions. The block diagram of the battery cycle aging test setup is given in Figure 6.

The Economic Battery Management System Subunit aims to conduct cost analyzes to ensure that battery systems are economically sustainable and to develop strategies to increase the economic value of energy storage projects. In addition, it is a system that will analyze the market values and price projections of second-life batteries as they transition from the first life to the second life within the optimum time.

The Training Center is a subunit that aims to organize training programs on battery technologies and train qualified human resources in accordance with the needs of the
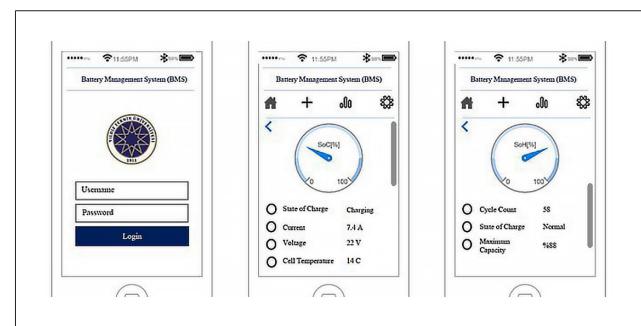

Figure 7. Conceptual mobile application interface.

sector. By creating modular, classified training contents and plans, a training center will be established to meet the employment needs for the private sector and the public, including technical personnel at all levels, as well as manager and planner levels.

The Awareness Center is a subunit that aims to increase the society's knowledge about the benefits, use, recycling and sustainability of battery technologies. By informing the society about the mentioned issues, this center will extend the average battery life in the country and will also raise awareness in the relevant sectors about sustainability-supporting practices such as recycling and second use.

In the final stage, all data regarding the SoH and optimum sizing of the battery will be presented as output by developing a software. The mobile application, which can run on both Android and iOS platforms, will create a user interface in this context. The interface will be designed by creating a user experience in which even people who are unfamiliar with technology can easily use the application. On the first page of the application, the user will be asked for login information to enter the system. On the other screen, the user will be able to examine technical values such as SoC and SoH values of the storage device, charge and discharge status, current, voltage, cell temperature, total number of cycles, whether the storage device is usable or not, and the status of its maximum capacity. A conceptual mobile application interface is given in Figure 7.

By establishing these subunits, it is aimed to achieve goals such as developing battery technologies, increasing performance, determining safety standards, ensuring economic sustainability, training qualified human resources and raising public awareness. These subunits will contribute to the country's leading position by supporting innovations in battery technologies and will enable an important step towards the sustainable energy future.

CONCLUSION

As global demand for energy storage continues to rise alongside the proliferation of EVs and renewable energy sources, the challenges of battery lifecycle management have
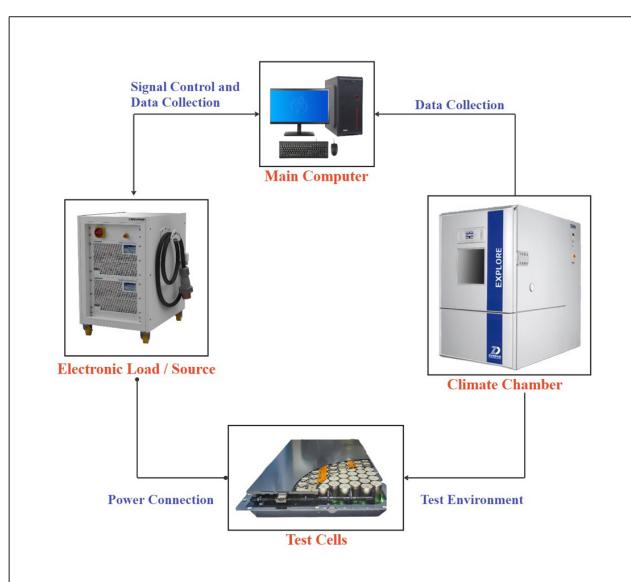
Figure 6. The block diagram of battery cycle aging test.

become increasingly critical. Conventional battery recycling methods, while essential, remain limited in scale and efficiency, often failing to fully address the economic and environmental consequences of EOL batteries. In this context, second-life applications emerge as a highly viable and sustainable alternative that not only extends battery lifespan but also significantly reduces waste and resource consumption.

This paper presents an overview of major battery technologies and emphasizes the growing need for second-life battery usage. The proposed laboratory, with its advanced technological infrastructure and specialized subunits, aims to establish a unique ecosystem that facilitates the reuse of EOL batteries in various applications, from ESS to small-scale mobility solutions. The laboratory's holistic design—including its focus on aging analysis, battery design optimization, smart BMS integration, economic evaluation, and data management—ensures that batteries can be repurposed safely and efficiently. Moreover, by bridging academic research and industrial needs, the lab supports the development of standards and practical solutions suited to real-world challenges.

AUTHORSHIP CONTRIBUTIONS

Authors equally contributed to this work.

DATA AVAILABILITY STATEMENT

The authors confirm that the data that support the findings of this study are available within the article. Raw data that support the finding of this study are available from the corresponding author, upon reasonable request.

CONFLICT OF INTEREST

The authors declared no potential conflicts of interest with respect to the research, authorship, and/or publication of this article.

ETHICS

There are no ethical issues with the publication of this manuscript.

STATEMENT ON THE USE OF ARTIFICIAL INTELLIGENCE

Artificial intelligence was not used in the preparation of the article.

REFERENCES

[1] Worku MY. Recent advances in energy storage systems for renewable source grid integration: A comprehensive review. Sustainable 2022;14:5985. [CrossRef]

[2] Rey SO, Romero JA, Romero LT, Martinez AF, Roger XS, Qamar MA, et al. Powering the future: A comprehensive review of battery energy storage systems. Energies 2023;16:6344. [CrossRef]

[3] Ranjith Kumar R, Bharatiraja C, Udhayakumar K, Devakirubakaran S, Sekar KS, Mihet-Popa L. Advances in batteries, battery modeling, battery management system, battery thermal management, SOC, SOH, and charge/discharge characteristics in EV applications. IEEE Access 2023;11:105761–105809. [CrossRef]

[4] May GJ, Davidson A, Monahov B. Lead batteries for utility energy storage: A review. J Energy Storage 2018;15:145–157. [CrossRef]

[5] Deng D. Li-ion batteries: Basics, progress, and challenges. Energy Sci Eng 2015;3:385–418.

[6] Goodenough JB, Park KS. The Li-ion rechargeable battery: A perspective. J Am Chem Soc 2013;135:1167–1176. [CrossRef]

[7] Shukla AK, Venugopalan S, Hariprakash B. Nickel-based rechargeable batteries. J Power Sources 2001;100:125–148.

[8] Pistoia G, Liaw B. Behaviour of lithium-ion batteries in electric vehicles. 2018.

[9] Khawaja Y, Shankar N, Qiqieh I, Alzubi J, Alzubi O, Nallakaruppan MK, et al. Battery management solutions for li-ion batteries based on artificial intelligence. Ain Shams Eng J 2023;14:102213. [CrossRef]

[10] Lv Y, Huang S, Zhao Y, Roy S, Lu X, Hou Y, et al. A review of nickel-rich layered oxide cathodes: Synthetic strategies, structural characteristics, failure mechanism, improvement approaches and prospects. Appl Energy 2022;305:117849. [CrossRef]

[11] Li F, Liu Q, Hu J, Feng Y, He P, Ma J. Recent advances in cathode materials for rechargeable lithium-sulfur batteries. Nanoscale 2019;11:15418–15439. [CrossRef]

[12] Purwanto A, Yudha CS, Ubaidillah U, Widiyandari H, Ogi T, Haerudin H. NCA cathode material: Synthesis methods and performance enhancement efforts. Mater Res Express 2018;5:125507. [CrossRef]

[13] Alikin D, Slautin B, Kholkin A. Revealing lithiation kinetics and battery degradation pathway in LiMn2O4-based commercial cathodes via electrochemical strain microscopy. Batteries 2022;8:220. [CrossRef]

[14] Han X, Ouyang M, Lu L, Li J. Cycle life of commercial lithium-ion batteries with lithium titanium oxide anodes in electric vehicles. Energies 2014;7:4895–4909. [CrossRef]

[15] Lu Y, Zhang Y, Zhang Q, Cheng F, Chen J. Recent advances in Ni-rich layered oxide particle materials for lithium-ion batteries. Particuology 2020;53:1–11. [CrossRef]

[16] Wu Z, Christofides PD. Economic machine-learning-based predictive control of nonlinear systems.

Mathematics 2019;7:494. [CrossRef]

[17] Engel GS, Hertzke P. Second-life EV batteries: The newest value pool in energy storage. İstanbul: McKinsey & Company; 2019.

[18] Li S, Sun F, He H, Chen Y. Optimization for a grid-connected hybrid PV-wind-retired HEV battery microgrid system. Energy Proced 2017;105:1634–1643. [CrossRef]

[19] Dong Q, Liang S, Li J, Kim HC, Shen W, Wallington TJ. Cost, energy, and carbon footprint benefits of second-life electric vehicle battery use. iScience 2023;26:107195. [CrossRef]

[20] Hamidi A, Weber L, Nasiri A. EV charging station integrating renewable energy and second-life battery. Proc Int Conf Renew Energy Res Appl 2013:1217–1221. [CrossRef]

[21] Alhadri M, Zakri W, Esmaeeli R, Mohammed AH, Hashemi SR, Barua H, et al. Analysis of second-life of a lithium-ion battery in an energy storage system connected to a wind turbine. 2019 IEEE Power and Energy Conference at Illinois (PECI), Champaign, IL, USA, 2019, pp. 1–8. [CrossRef]

[22] BYD. Your battery partner. 2022. Available at: https://www.bydbatterybox.com/news Accessed Feb 02, 2026.

[23] Saez-De-Ibarra A, Martinez-Laserna E, Koch-Ciobotaru C, Rodriguez P, Stroe DI, Swierczynski M. Second life battery energy storage system for residential demand response service. Proc IEEE Int Conf Ind Technol 2015:2941–2948. [CrossRef]

[24] Saez-De-Ibarra A, Martinez-Laserna E, Stroe DI, Swierczynski M, Rodriguez P. Sizing study of second life li-ion batteries for enhancing renewable energy grid integration. IEEE Trans Ind Appl 2016;52:4999–5007. [CrossRef]

[25] Leung C. PV systems with second life li-ion battery technology (Master thesis). Murdoch, Australia: Murdoch University Division of Science and Engineering; 2012.

[26] Fitzpatrick A. Electric car batteries get a second life storing solar power. Axios 2023. Avaialble at: https://www.axios.com/2023/02/07/electric-car-batteries-solar-power-storage Accessed on Feb 02, 2026. [CrossRef]

[27] Neubauer J, Smith K, Wood E, Pesaran A. Identifying and overcoming critical barriers to widespread second use of PEV batteries. Natl Renew Energy Lab 2015:23–62. [CrossRef]

[28] Lacey G, Putrus G, Salim A. The use of second life electric vehicle batteries for grid support. IEEE EuroCon 2013:1255–1261. [CrossRef]

[29] Eyer J, Corey G. Energy Storage for the Electricity grid: Benefits and Market Potential Assessment Guide. Virginia, USA: Sandia National Laboratories; 2011. p. 1–191. [CrossRef]

[30] Liang L. Research on electric vehicle lithium battery retired echelon use in communication base station. Heilongjiang, China: Harbin Institute of Technology; 2018.

[31] Yan Z. Design of base station backup power system constructed with ladder battery. IOP Conf Ser Mater Sci Eng 2019;677:032011. [CrossRef]

[32] Dongsheng J, Jinguo Z, Jie Z, Zhongjun C, Xianglong L. Economic operation analysis of energy storage system based on echelon-use batteries. 2014 China International Conference on Electricity Distribution (CICED), Shenzhen, 2014, pp. 499–503. [CrossRef]

[33] Han X, Liang Y, Ai Y, Li J. Economic evaluation of a PV combined energy storage charging station based on cost estimation of second-use batteries. Energy 2018;165:326–339. [CrossRef]

[34] Kamath D, Arsenault R, Kim HC, Anctil A. Economic and environmental feasibility of second-life lithium-ion batteries as fast-charging energy storage. Environ Sci Technol 2020;54:6878–6887. [CrossRef]

[35] Potevio New Energy. Exploring mobile charging projects via echelon use of retired batteries. 2017.

[36] Schmidt B. Camping gets a recharge with second-life Nissan EV batteries. The Driven 2019.

[37] Zhang GMTP, Yang F, Tang W, Alexander M, Forastiere L, Kumar N, et al. Analysis of the development of the new energy vehicle power battery echelon use industry. Infect Dis Poverty 2019;8:76–78.

[38] Zhao G. Resource utilization and harmless treatment of power batteries. 2017.

[39] Zhu QJM, Wu Z, Huang Y, Zhou S. Analysis of the application of echelon use batteries in solar streetlights. Sol Energy 2020;2:56–60.

[40] Canals Casals L, Amante García B, González Benítez MM. Aging model for re-used electric vehicle batteries in second life stationary applications. 2017:139–151. [CrossRef]

[41] Neubauer JEJ, Pesaran A, Williams B, Ferry M. Techno-economic analysis of PEV battery second use: Repurposed-battery selling price and commercial and industrial end-user value. SAE Technical Paper 2012-01-0349, 2012. [CrossRef]

[42] Streb M, Ohrelius M, Klett M, Lindbergh G. Improving Li-ion battery parameter estimation by global optimal experiment design. J Energy Storage 2022;56:105948. [CrossRef]

[43] Lai X, Huang Y, Gu H, Deng C, Han X, Feng X, et al. Turning waste into wealth: A systematic review on echelon utilization and material recycling of retired lithium-ion batteries. Energy Storage Mater 2021;40:96–123. [CrossRef]

[44] Nováková K, Pražanová A, Stroe DI, Knap V. Second-life of lithium-ion batteries from electric vehi-

cles: Concept, aging, testing, and applications. Energies 2023;16:2345. [CrossRef]

[45] Hossain E, Murtaugh D, Mody J, Faruque HMR, Sunny MSH, Mohammad N. A comprehensive review on second-life batteries: Current state, manufacturing considerations, applications, impacts, barriers potential solutions, business strategies, and policies. IEEE Access 2019;7:73215–73252. [CrossRef]